NAVAL POSTGRADUATE SCHOOL
Monterey, California

THESIS

DESIGN AND COLD-FLOW EVALUATION OF A MINIATURE MACH 4 RAMJET

by

Kevin M. Ferguson

June 2003

Thesis Advisor:	Garth V. Hobson
Second Reader:	Raymond P. Shreeve

THIS PAGE INTENTIONALLY LEFT BLANK

REPORT DOCUMENTATION PAGE			Form Approved OMB No. 0704-0188
Public reporting burden for this collection of information is estimated to average 1 hour per response, including the time for reviewing instruction, searching existing data sources, gathering and maintaining the data needed, and completing and reviewing the collection of information. Send comments regarding this burden estimate or any other aspect of this collection of information, including suggestions for reducing this burden, to Washington headquarters Services, Directorate for Information Operations and Reports, 1215 Jefferson Davis Highway, Suite 1204, Arlington, VA 22202-4302, and to the Office of Management and Budget, Paperwork Reduction Project (0704-0188) Washington DC 20503.			
1. AGENCY USE ONLY *(Leave blank)*	**2. REPORT DATE** June 2003	**3. REPORT TYPE AND DATES COVERED** Master's Thesis	
4. TITLE AND SUBTITLE: Design and Cold Flow Evaluation of a Miniature Mach 4 Ramjet			**5. FUNDING NUMBERS**
6. AUTHOR(S) Kevin M. Ferguson			
7. PERFORMING ORGANIZATION NAME(S) AND ADDRESS(ES) Naval Postgraduate School Monterey, CA 93943-5000			**8. PERFORMING ORGANIZATION REPORT NUMBER**
9. SPONSORING /MONITORING AGENCY NAME(S) AND ADDRESS(ES) N/A			**10. SPONSORING/MONITORING AGENCY REPORT NUMBER**
11. SUPPLEMENTARY NOTES The views expressed in this thesis are those of the author and do not reflect the official policy or position of the Department of Defense or the U.S. Government.			
12a. DISTRIBUTION / AVAILABILITY STATEMENT Approved for public release; distribution is unlimited			**12b. DISTRIBUTION CODE**

13. ABSTRACT ***(maximum 200 words)***

Methods used for designing the ramjet included conic shock tables; isentropic flow tables and the GASTURB code was used for aerothermodynamic performance prediction. The flow field through the proposed geometry was computed using the OVERFLOW code, and small modifications were made. Geometry and solid models were created and built using SolidWorks 3D solid modeling software. A prototype ramjet was manufactured with wind tunnel mounting struts capable of measuring axial force on the model. Shadowgraph photography was used in the Mach 4 supersonic wind tunnel at the Naval Postgraduate School's Turbopropulsion Laboratory to verify predicted shock placement, and surface flow visualization was obtained of the airflow from fuel injection ports on the inlet cone of the model. All indications are that the cold-flow tests were successful.

14. SUBJECT TERMS Ramjet, GASTURB, OVERFLOW, SolidWorks, Shadowgraph, Computation Fluid Dynamics, Stagnation Pressure Ratio, Inlet Cone Angle			**15. NUMBER OF PAGES** 85
			16. PRICE CODE
17. SECURITY CLASSIFICATION OF REPORT Unclassified	**18. SECURITY CLASSIFICATION OF THIS PAGE** Unclassified	**19. SECURITY CLASSIFICATION OF ABSTRACT** Unclassified	**20. LIMITATION OF ABSTRACT** UL

NSN 7540-01-280-5500

Standard Form 298 (Rev. 2-89)
Prescribed by ANSI Std. 239-18

THIS PAGE INTENTIONALLY LEFT BLANK

Approved for public release; distribution is unlimited

DESIGN AND COLD-FLOW EVALUATION OF A MINIATURE MACH 4 RAMJET

Kevin M. Ferguson
Ensign, United States Naval Reserve
B.S., Massachusetts Institute of Technology, 2002

Submitted in partial fulfillment of the
requirements for the degree of

MASTER OF SCIENCE IN AERONAUTICAL ENGINEERING

from the

NAVAL POSTGRADUATE SCHOOL
June 2003

Author: Kevin M. Ferguson

Approved by: Garth V. Hobson
Thesis Advisor

Raymond P. Shreeve
Second Reader

Max F. Platzer
Chair, Department of Aeronautics

THIS PAGE INTENTIONALLY LEFT BLANK

ABSTRACT

Methods used for designing the ramjet included conic shock tables; isentropic flow tables and the GASTURB code was used for aerothermodynamic performance prediction. The flow field through the proposed geometry was computed using the OVERFLOW code, and small modifications were made. Geometry and solid models were created and built using SolidWorks 3D solid modeling software. A prototype ramjet was manufactured with wind tunnel mounting struts capable of measuring axial force on the model. Shadowgraph photography was used in the Mach 4 supersonic wind tunnel at the Naval Postgraduate School's Turbopropulsion Laboratory to verify predicted shock placement, and surface flow visualization was obtained of the airflow from fuel injection ports on the inlet cone of the model. All indications are that the cold-flow tests were successful.

THIS PAGE INTENTIONALLY LEFT BLANK

TABLE OF CONTENTS

LIST OF FIGURES

LIST OF TABLES

THIS PAGE INTENTIONALLY LEFT BLANK

ACKNOWLEDGMENTS

I would like to extend my wholehearted appreciation in acknowledging several people whose efforts greatly contributed to the successful completion of this thesis.

A great thanks extends to Frank Franzen from the Mechanical Engineering Machine Shop, who single-handedly built and assembled the smallest parts he had every made before. His quest for excellence enabled the successful fabrication and testing of the ramjet before too late.

Thanks to Mr. Rick Still, Mr. John Gibson, and Mr. Doug Seivwright at the Turbopropulsion Lab for their help and assistance with testing and evaluation. A special thanks goes out to Antony Ganon at the Turbopropulsion Lab for his help and guidance through the everyday struggle of research and development.

Most notable thanks to my advisor Dr. Garth Hobson of the Department of Aeronautics and Astronautics for affording the opportunity to work with him and his wonderful ideas. His driving endurance and focused guidance enabled the motivation for this research.

THIS PAGE INTENTIONALLY LEFT BLANK

I. INTRODUCTION

Air-breathing propulsion has been at the forefront of military science and technology programs since the first gas turbine was invented over 60 years ago. Existing air-breathing engine types are being continuously re-engineered and aerothermodynamically optimized to provide the lightest and most efficient power source. Depending on the desired operating speed of the engine, certain designs have proven the most efficient (Figure 1). At subsonic speeds, turbofans engines are best. With an increase in flight Mach number the relative mechanical complexity decreases but the geometric and aerothermodynamic complexity increases dramatically. The variable-cycle turbofan, the most mechanically challenging gas turbine, gives way to the turbojet, ramjet, and finally at the highest Mach numbers, the supersonic combustion ramjet, or scramjet. The target flight regime for this thesis was Mach 4 and the design and analysis of a miniature ramjet was undertaken.

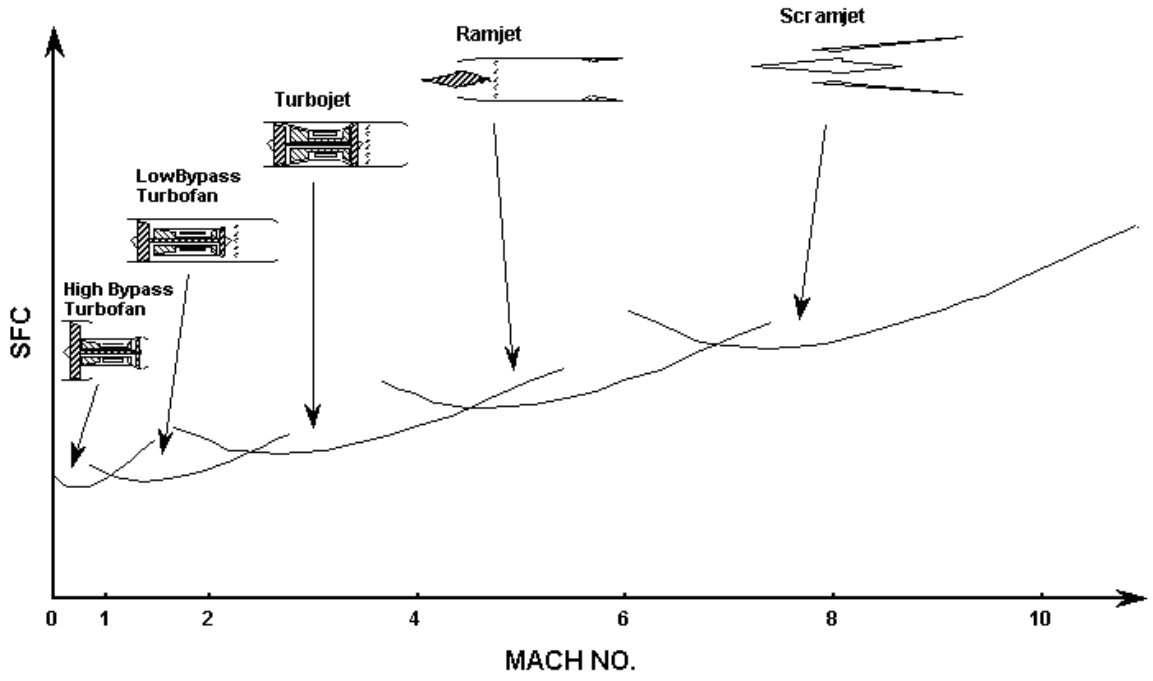

Figure 1. SFC vs. Mach number for air-breathing engines.

In 1998 [ref. 1], work at the Naval Postgraduate School's (NPS) Turbopropulsion Laboratory (TPL) was started to design and develop a turbo-ramjet engine that combined both the mechanical compression of turbojet machinery with the geometrical natural compression of a ramjet. This engine was intended for Mach 2. It was tested successfully at subsonic conditions in early 2003 [ref. 2] with the addition of an afterburner.

The next step was to undertake a Mach 4 air breathing engine design. The ramjet was chosen for its simplicity and good performance at high supersonic speeds. Additionally, the facilities at TPL included a Mach 4 supersonic blow-down wind tunnel. Since the wind tunnel had a 4 x 4 inch test section, the resulting ramjet could only be about 1 inch in diameter. However, the small scale of the ramjet kept the cost of manufacturing and testing relatively low. Possible applications for such a ramjet include use in small supersonic missiles, or more likely, high speed guided projectiles.

Currently, there is no available data set for performance measurements at Mach 4 in the open literature. The present project was intended to create such a data set. The objective was to design, analyze computationally, and test a working Mach 4 miniature ramjet. Ultimately this small engine will be flight tested using a gun to launch the ramjet close to its flight speed, where it will the ignite and provide its own thrust for cruise at Mach 4.

II. DESIGN

A. METHODOLOGY

At the outset, a decision was made to design an axisymmetric ramjet with conical inlet, as this resulted in the most efficient design with respect to inlet total pressure recovery. Additionally it also resulted in ease of manufacturing, as the inlet, combustor and nozzle would be machined on a lathe.

Design of the miniature ramjet was an iterative process. Before the iterations could begin, a number of conical shock flow calculations were carried out. Shock angles, pressure ratios, and area ratios were computed and the results are compiled in Appendix A. The summary plot of the calculations is shown in Figure 2. The graph shows the optimum total pressure recovery ratio versus Mach number (from 2-4) and cone angle (from 2.5-30 degrees).

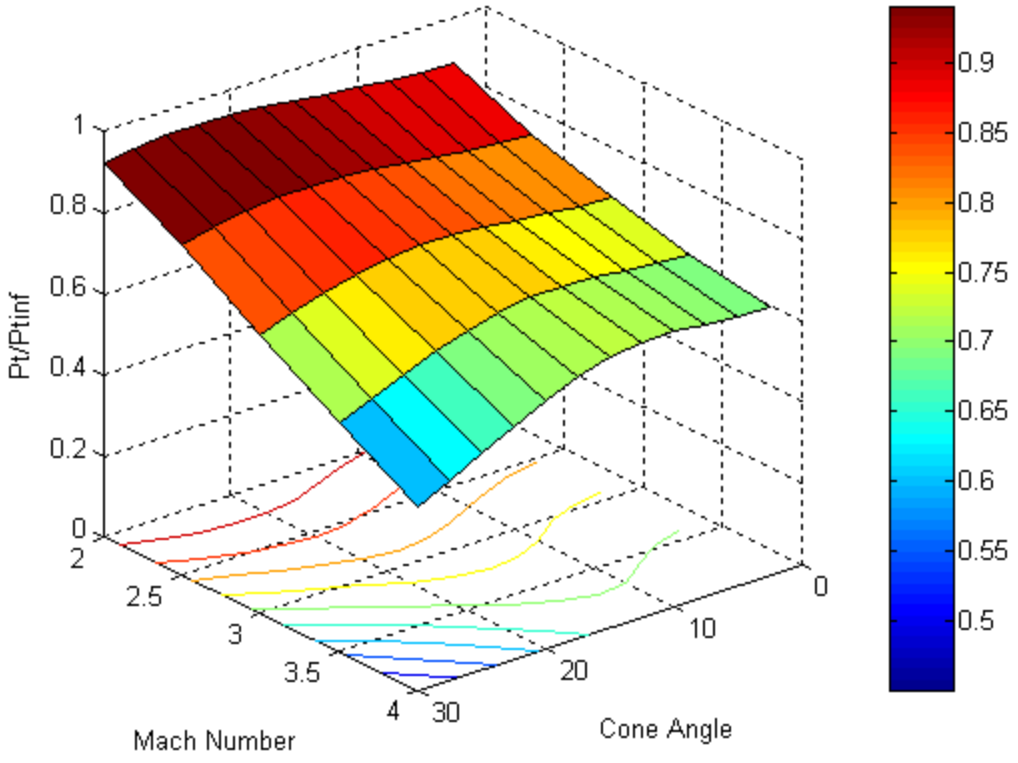

Figure 2. Normal shock recovery pressure ratio vs. Mach number and cone angle

Also crucial to the design was the diameter of the ramjet, driven by the dimensions of the wind tunnel. Additionally, the overall length of the intake cone was to be kept reasonable. The details of each step will be explained in the following sections. A sample calculation of the external compression process is given in Appendix B.

The spreadsheet in Appendix C was set-up and used to begin the iterative design process. First an inlet cone angle was chosen based on maximum total pressure recovery. The geometry of the inlet was then defined by positioning the oblique shock on the lip of the cowling. The combustion chamber entrance Mach number was selected and the resulting cross-sectional area of the combustor was calculated. Next, this area was used to determine the necessary inlet area, which then sized the dimensions of the lip of the inlet cowl. Given these dimensions an inlet air mass-flow rate was calculated and compared to the mass-flow rate input into GASTURB [ref. 3]. If more air mass-flow rate was needed, the inlet was made larger, and the cone angle was adjusted thereby repeating the process again. The final GASTURB input and output files are shown in Table 1 and Table 2. The stations associated to the numbers in the tables are shown in Figure 3. The fuel used for the initial design was methane, although other fuels were investigated, including hydrogen, propane, JP-10, and kerosene. The results of this study are shown in Appendix D.

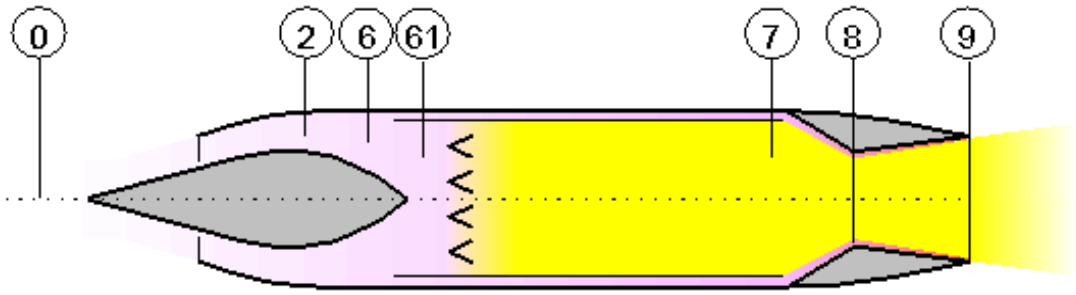

Figure 3. GASTURB diagram of ramjet showing station locations

Altitude	ft	59055.12
Delta T from ISA	R	0
Relative Humidity [%]		0
Mach Number		4
Inlet Corr. Flow W2Rstd	lb/s	0.0959139
Intake Pressure Ratio P2/P1		0.664
Diffuser Pressure Ratio P6/P2		0.97
Burner Exit Temperature	R	4320
Burner Efficiency		0.95
Fuel Heating Value	BTU/lb	23231.36
Nozzle Cooling Air Wcl/W6		0.04
Burner Inlet Mach Number		0.15
Nozzle Thrust Coefficient		1
Con-Di Nozzle:		
Nozzle Area Ratio		2.5972

Table 1. GASTURB design point input data.

Station	W	T	P	WRstd	FN	=	32.02
amb		389.97	1.088		SFC	=	1.9709
1		1588.4	171.072		WF	=	0.01753
2	0.424	1588.4	113.592	0.096	FN/W2	=	2432.0296
61	0.407	1588.4	110.184		P2/P1	=	0.6640
7	0.424	4320.00	106.754		A8	=	0.5229
8	0.441	4218.7	106.754		P8/Pamb	=	98.0755
Burner Efficiency			0.9500		A61	=	1.10288
Jetpipe Diam.			1.1850		XM6	=	0.15000
Pressure Loss [%]			3.11		XM7	=	0.28392
Con-Di Nozzle:					A9/A8	=	2.59754
A9*(Ps9-Pamb)			8.933		XM9	=	2.34822
					CFGid	=	0.93320

Table 2. GASTURB predicted design point performance using methane.

The overall design consisted of 5 main sections: (1) Center body, (2) Struts, (3) Intake, (4) Combustion Tube, and (5) Nozzle. The overall design is shown in below Figure 4 and will be discussed in detail in the following sections.

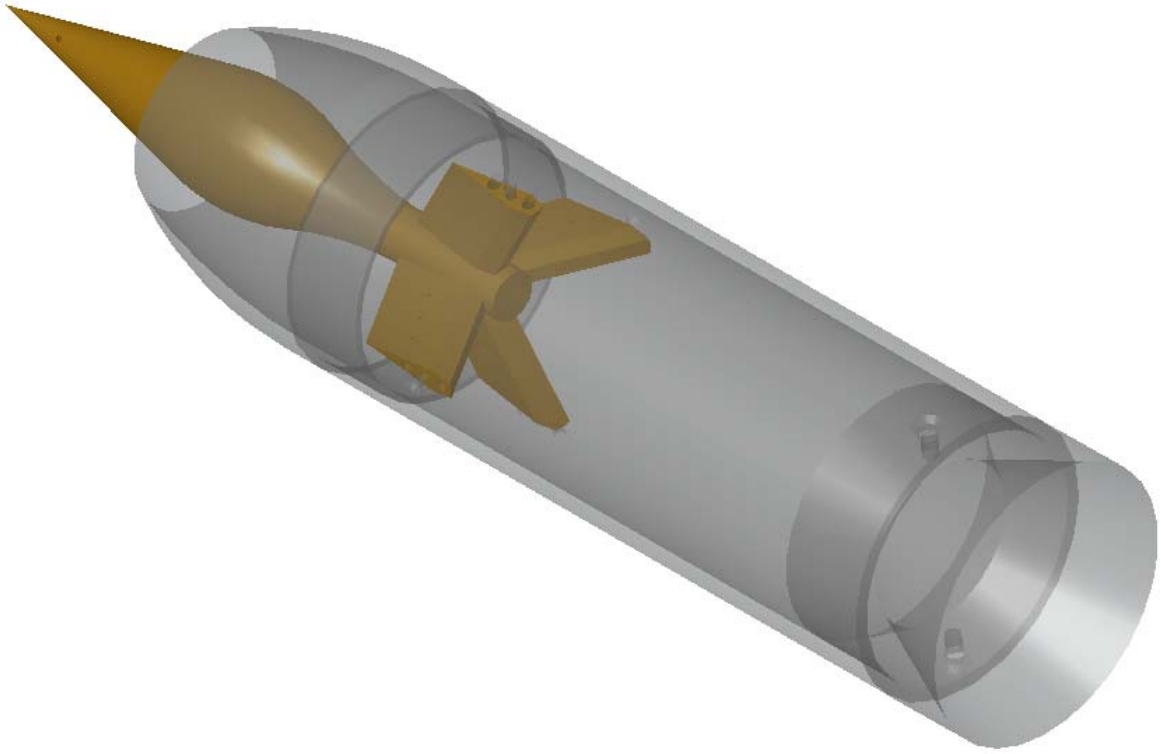

Figure 4. Assembled ramjet showing all parts. Image from SolidWorks.

B. INLET CONE ANGLE DETERMINATION

To keep the design simple, it was decided to design a two-shock (one oblique, one normal) external compression inlet with a specific inlet cone angle. The inlet cone angle was defined as the half angle between the axis of revolution of the cone and surface of the cone (Figure 5). A parametric study was conducted to determine the optimal angle for the ramjet. Table 3 and Figure 6 and show the results of this study at Mach 4.0. The optimal cone angle produced the largest stagnation pressure recovery ratio ($Pt2/Pt_\infty$). The full study covered the Mach number range from 2-4 and is attached as Appendix A. A sample calculation is shown in Appendix B. The cone angles were found using NASA conical shock tables [ref. 4] and isentropic flow tables [ref. 5]. By fitting a 6^{th} order polynomial through the calculated stagnation pressure ratio points vs. inlet cone angle (Figure 6), the optimal cone angle was determined to be 11.367 degrees at the design Mach of 4.0. This angle was not used for the final design however. It was necessary to increase this angle slightly in order to shorten the overall dimension of the cone. The final cone angle was 12.5 degrees, offering a compromise as a shorter cone with a minimal reduction in stagnation pressure recovery ratio.

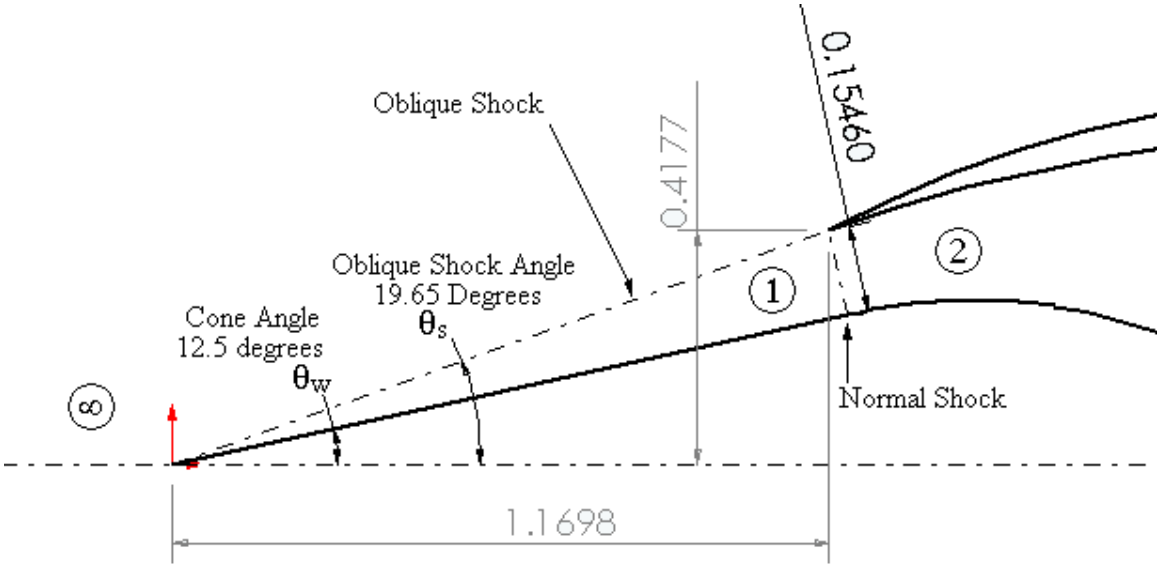

Figure 5. Inlet cone angle and associated dimensions.

Mach 4

Cone Angle	Oblique Shock Angle	Pressure Recovery Ratio
2.5	14.51	0.659
5.0	14.96	0.659
7.5	16.09	0.667
10.0	17.71	**0.677**
12.5	19.65	**0.676**
15.0	21.79	0.664
17.5	24.08	0.644
20.0	26.49	0.611
22.5	28.98	0.570
25.0	31.56	0.534
27.5	34.21	0.492
30.0	36.94	0.451

Table 3. Intake stagnation pressure ratio at Mach 4 with various cone angles and associated oblique shock angles.

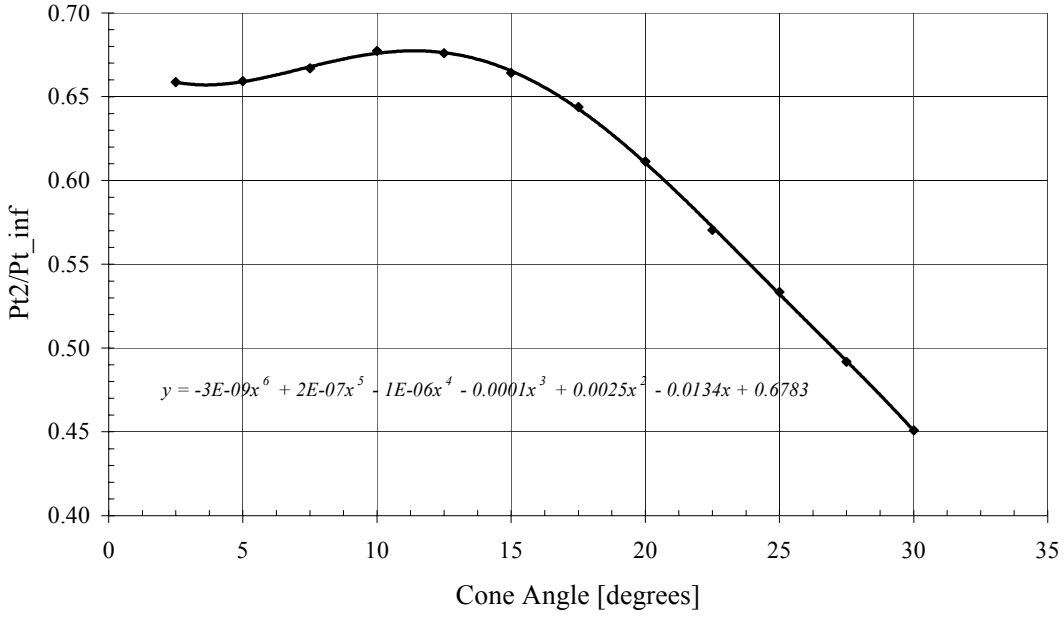

Figure 6. Inlet recovery stagnation pressure ratio of intake as a function of cone angle.

C. INLET GEOMETRY

Designing the inlet geometry was the most critical aspect of the ramjet design. If the inlet was not correctly sized, the oblique and normal shocks would not sit in the right place and a large reduction in pressure recovery ratio would occur. This would result in greatly reduced thrust from a reduction in mass flow rate and/or increased drag from the formation of additional shocks.

The inlet area was calculated during the iterative process after the combustor area and diffuser exit Mach number were determined. The inlet area was calculated using the isentropic flow tables [ref. 5]. The affects of different Mach numbers and different cone angles on inlet area are shown in Appendix C.

After the inlet area was determined, the lip of the intake was positioned. The vertical dimension of the lip was positioned so that the oblique shock shed from the cone tip would sit on the lip of the intake (Figure 5). As a check on the dimensions of the lip, SolidWorks was used to verify that the lip and cone positions gave the appropriate intake area.

In conjunction with the inlet, the downstream subsonic diffuser geometry was critically important to properly expand the incoming air from Mach 0.5 to Mach 0.15. If the air were expanded too rapidly, separation bubbles would occur that would choke the flow and affect the normal shock. Figure 7 shows a sketch of the diffuser contour. The initial dimensions of the diffuser are shown, which were altered after the CFD solutions were obtained.

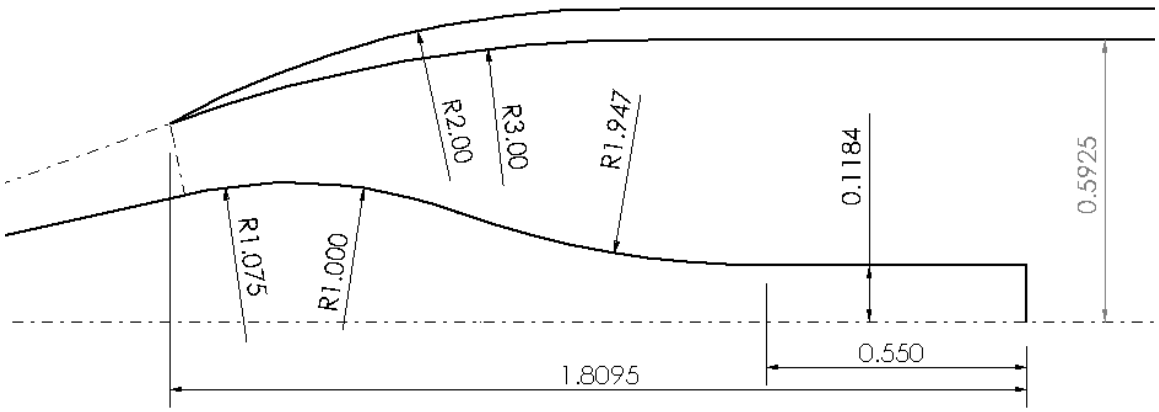

Figure 7. Axisymmetric diffuser contour.

D. NOZZLE

The next dimensions to be determined were the nozzle throat and exit areas. After combustion, the gases were to be expanded using a convergent-divergent nozzle, which would maximize the thrust produced by the ramjet. Unfortunately, the exit area of the nozzle was not perfectly expanded because the nozzle exit area was determined by the overall diameter of the ramjet. Below are the characteristics of the nozzle found using GASTURB along with a SolidWorks picture (Figure 8).

- Throat Area 0.4869 in^2
- Throat Diameter 0.7874 in
- Nozzle Exit Area 1.3581 in^2
- Nozzle Area Ratio 2.789

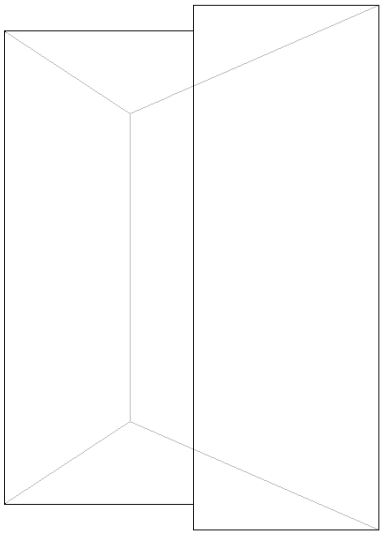

Figure 8. Side view of convergent-divergent nozzle.

The nozzle was designed to be removable from the combustion chamber of the ramjet for testing and evaluation purposes. Additional nozzles could easily be designed and built for testing with the rest of the ramjet to experimentally optimize the thrust.

E. FUEL SYSTEM

To generate the required fuel-air mixture and obtain the most thrust possible by, fuel injectors were placed in each of the four struts and also very close to the tip of the cone itself. The earlier fuel was introduced into the flow, the sooner mixing could begin. The fuel system of the ramjet followed the path shown below in Figure 9. Fuel was designed to be injected though the sidewalls of the wind tunnel into the horizontal struts.

The fuel passed through the horizontal struts and into the center body, through the rear port (Figure 9a). From the center body fuel then was designed to flow out of the tip injectors and into the vertical struts as shown in the bottom figure.

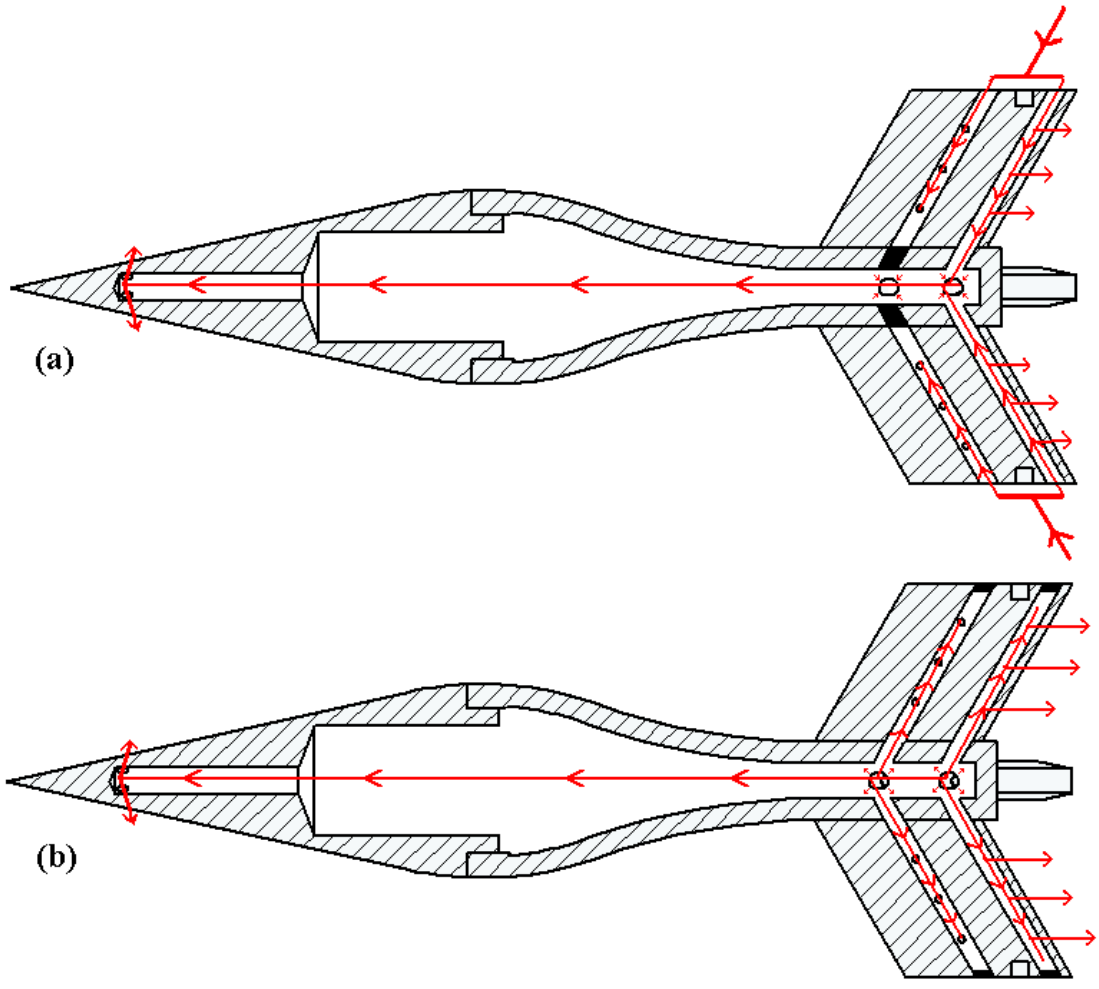

Figure 9. Diagram of fuel flow through horizontal plane (a) and vertical plane (b) of wind tunnel ramjet model.

1. Strut Injectors

The struts were designed to provide most of the fuel to the flow. As shown below (Figure 10), the struts had nine holes, each which contributed fuel. There were three holes on each side near the leading edge of each strut and three holes on the rear of each strut. The three holes at the rear of the struts could also be used as attachment points for flame holders. The positions and sizes would be subject to change in successive design iterations. Extensive testing and CFD would be required to determine the precise number and best location of each fuel injector port.

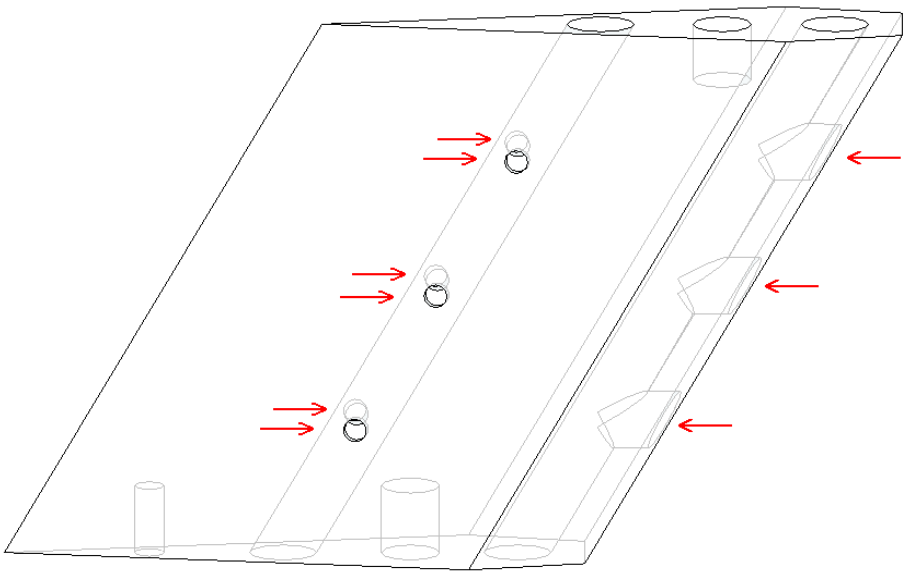

Figure 10. Side view of support strut. Fuel injection holes shown with arrows.

2. Cone Injectors

Additional fuel injection ports were added to the tip of the cone. This was done to introduce fuel into the flow of air as far forward as possible. The intent was to promote the longest mixing time between the fuel and the air before combustion. There were four injection ports placed near the tip of the cone, each 90 degrees from each other (Figure 11). The holes were placed such that they aligned with the middle of the spaces between the four struts, as shown in Figure 12.

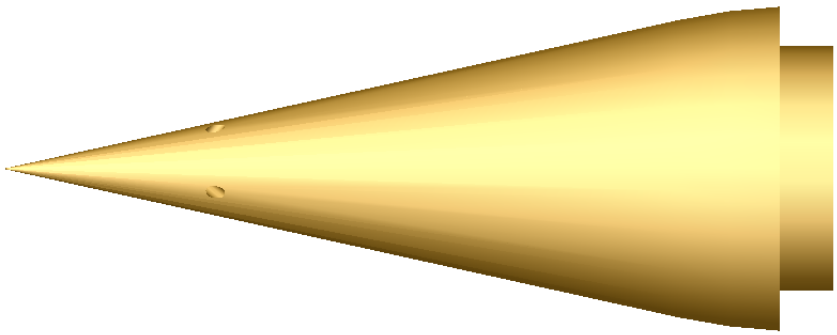

Figure 11. 3-D side view of inlet cone with 2 of 4 fuel injection holes shown.

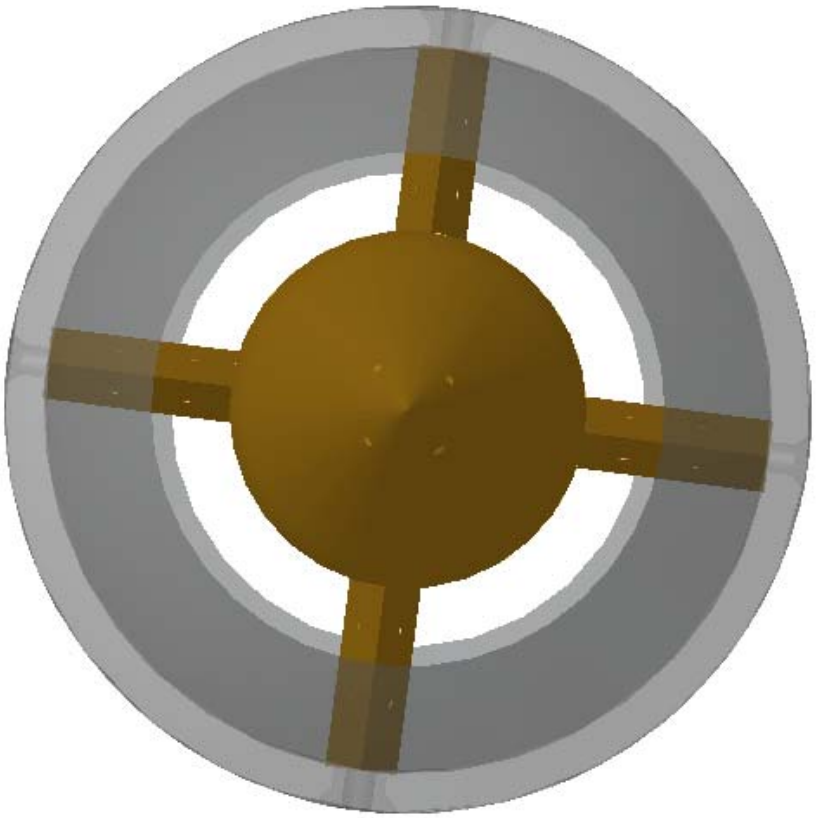

Figure 12. Front view of ramjet showing spacing of fuel injection holes on the inlet cone with respect to the support struts.

F. COMBUSTION CHAMBER

The combustion chamber was the least complicated of any of the parts of the ramjet. The chamber itself was simply a housing for the overall ramjet and a connector between the intake and the nozzle. Combustion, if suitably sustained, would occur throughout this space.

The length of the combustion chamber was chosen both to size the entire ramjet and to provide the necessary length for complete combustion. The chamber configuration was a 2.5:1 aspect ratio between the length and diameter of the chamber. Figure 13 shows the combustion chamber without attachments or fuel holes.

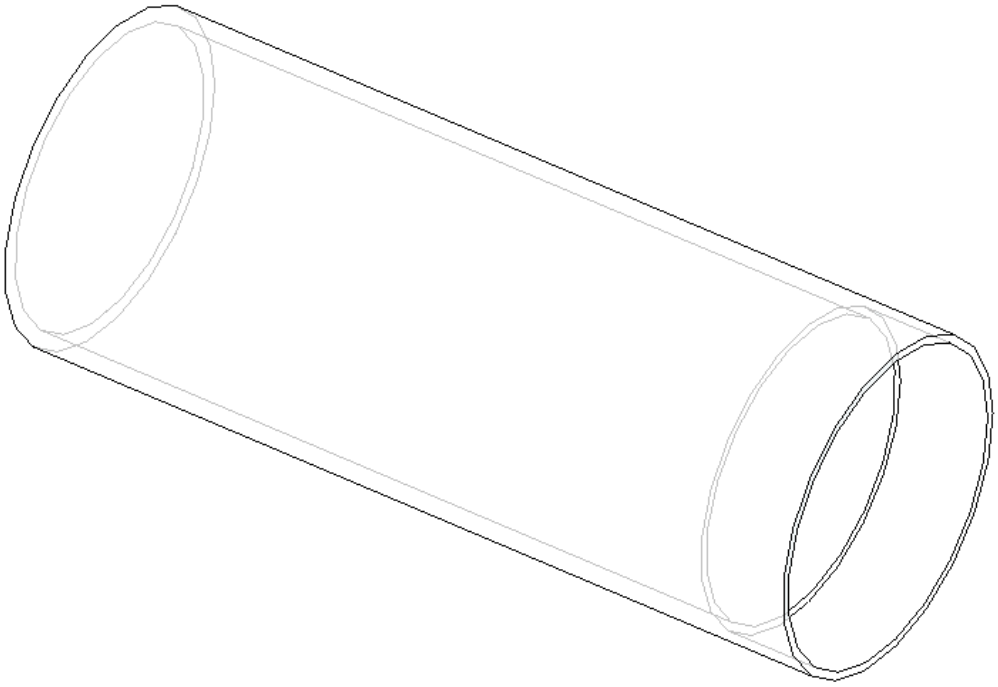

Figure 13. Combustion chamber with space for the inlet at the front (left) and the nozzle at the back (right).

G. ASSEMBLY

The assembly of the ramjet is shown in Figure 4 at the beginning of the Chapter and is shown below in an exploded view as Figure 14. Detailed part drawings are given in Appendix E and a list of fasteners is given in Appendix F.

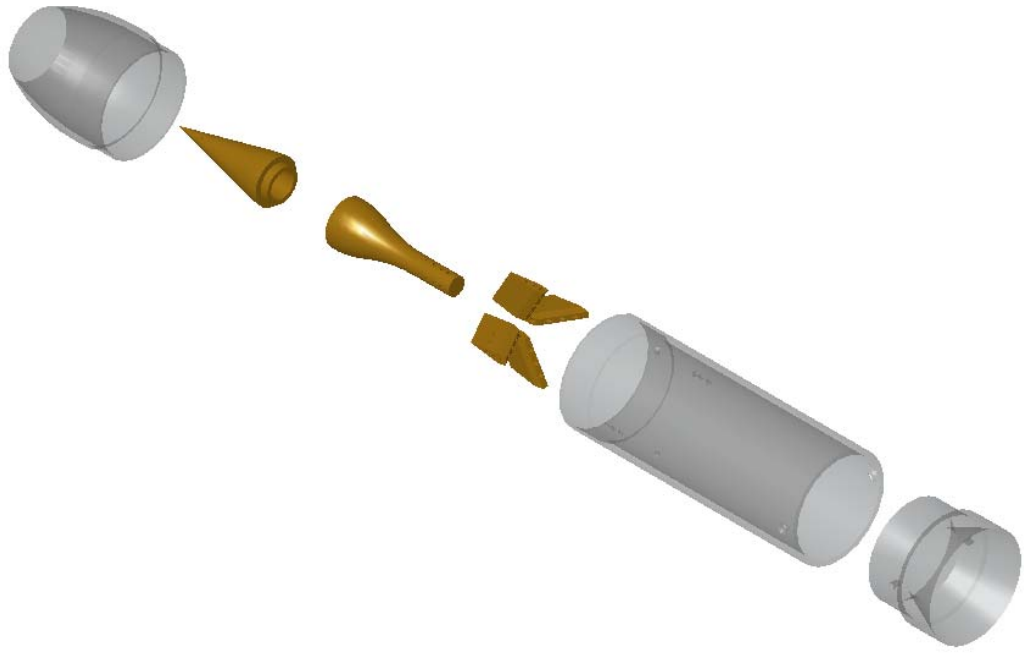

Figure 14. Exploded view of all parts of the ramjet. From left to right: intake, cone, cone rear, struts (4), combustion tube, and nozzle.

H. DESIGN TOOLS

The following computer software tools were used in the design of the ramjet:

- Microsoft Excel – used for iterative calculation and plotting.
- GASTURB 9.0 – Engine performance program developed by Joachim Kurzke; used for thermodynamics calculation and dimensioning.
- SolidWorks – Solid modeling package developed by the SolidWorks Corporation; used to model parts and create part drawings.
- OVERFLOW and FAST – CFD analysis and flow visualization software; used for further analysis and refinement.

THIS PAGE INTENTIONALLY LEFT BLANK

III. COMPUTATIONAL FLUID DYNAMICS (CFD)

CFD was used in parallel with the traditional design process to analyze the geometry of the ramjet and make subsequent changes if necessary. CFD is a computational approach to solving the complex systems of partial differential equations that describe flow fields. Approximated as finite differences, these equations can be iterated thousands of times by computer in matters of hours. The application of CFD techniques to solve for the flow over a known geometry is a well-developed process. Several software applications were used here for grid generation and refinement, and for flow analysis.

A. METHODOLOGY

The CFD process began by generating a grid based on the design geometry using GRIDGEN. Once the grid was developed, it was converted to the appropriate format using GRIDED for later use in the flow solution code OVERFLOW. After the solution was created, the residuals were plotted in GNUPLOT and the graphical analysis was done using FAST. The progression of the CFD was to begin with a viscous solution with only the inlet cone, outer duct and nozzle of the ramjet without combustion. Additionally an inviscid solution was run in parallel to the viscous solution. For the inviscid solution the nozzle area was decreased in an attempt to properly position the normal shock at the lip of the intake. Finally, heat was added to simulate combustion inside the ramjet.

B. DESIGN TOOLS AND RESULTS

1. GRIDGEN

GRIGDEN is a Computer Science Corporation developed software tool. It is an interactive code used to create two and three-dimensional grids. A 2D grid was created based on the geometry of the ramjet. The fineness of the grid depended on the relative gradients of the flow. These will be highest around all leading edges of the intake and along all the boundary layers within the ramjet. Figure 15 shows a part of a

representative grid used. The dark area represents the ramjet outer duct, which was blanked out as to simulate the thickness of the wall.

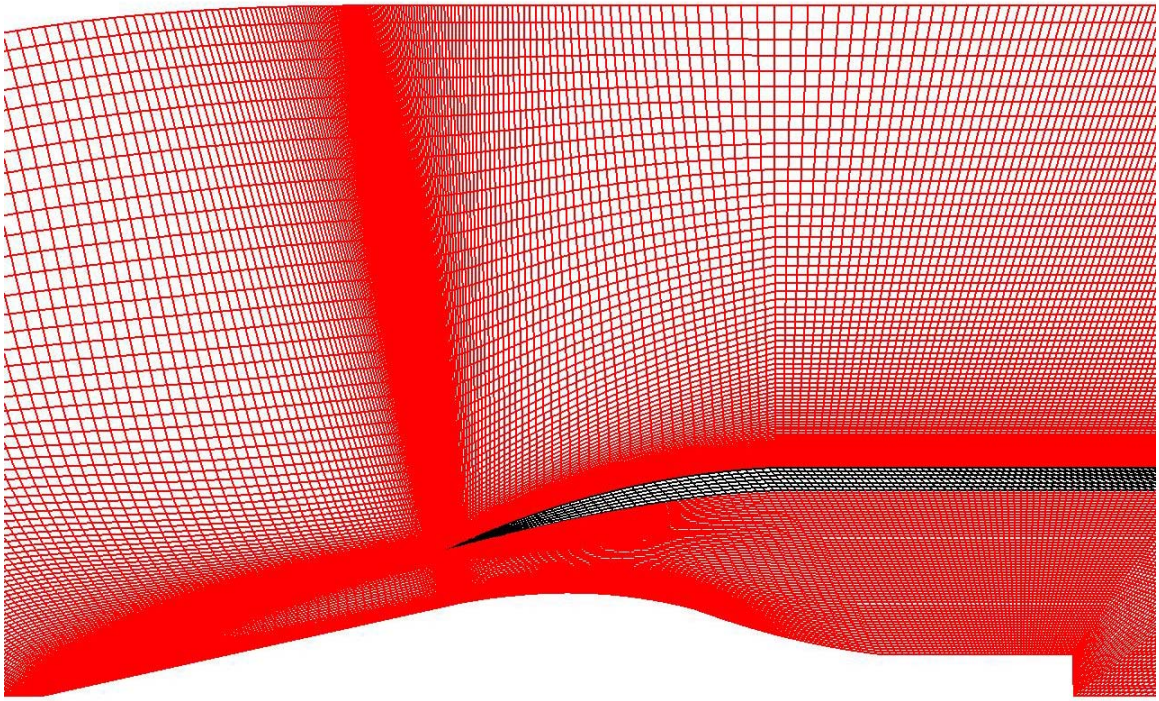

Figure 15. 431 x 147 x 3 grid created using GRIDGEN software

2. GRIDED

GRIDED is an interactive, menu-driven FORTRAN-based software application used to manipulate the grid that resulted from GRIDGEN. It was used to create a 3D axis-symmetric wedge from the given 2D plane. The 2D grid was rotated circumferentially by one degree in each direction creating a 3D grid necessary for OVERFLOW. A script of necessary commands is attached as Appendix G.

Before the grid could be read by OVERFLOW, it had to be converted from the ASCII output of GRIDED to binary format. This was done using the FORTRAN program xa2b.f.

3. OVERFLOW

OVERFLOW is a flow analysis code that was developed by NASA Ames Research Center. It used an implicit finite-differencing scheme to solve the Reynolds-Averaged Navier-Stokes equations in strong conservative form [ref. 6]. The input file was a user-generated file that enabled the selection of many options (Appendix H), the options pertinent to the viscous solution were:

- Flight regime or flow conditions, including Mach number (4.0) , Reynolds Number (2.3E6), and free stream temperature (122.4 R).
- Turbulence model selection (options include Baldwin-Lomax, Baldwin-Barth and k-ϖ models, with the latter chosen for the viscous solutions)
- Computational controls such as time step, difference scheme, artificial viscosity selection and smoothing parameters.
- Boundary conditions (options include viscous or inviscid walls, inflow/outflow, constant temperature walls, axis-symmetric lines, etc.).

In OVERFLOW, many different models were tried. First, the design geometry was tried using a standard grid with viscous walls. From this model a prediction of the drag coefficient of the ramjet was calculated to be 0.0193 with a resulting drag of 4.80 lbs. Next an inviscid solution was run to investigate whether a change in nozzle area would affect the position of the normal shock within the intake.

The next models tried were to more realistically model the physics that would occur in the ramjet. First heat was added to the internal walls of the ramjet to simulation combustion (Appendix I). Next the model was tried without the heat, but with air flowing from the tip of the nose cone. This was to simulate fuel flowing from the cone and to determine its affect on the flow.

4. GNUPLOT

This program is a UNIX-based plotting program that graphically displays data. It was used to display residual decay with an increase in the number of iterations performed. The representative plot of the residuals is shown in Figure 16.

Figure 16 was created for the present publication using MATLAB.

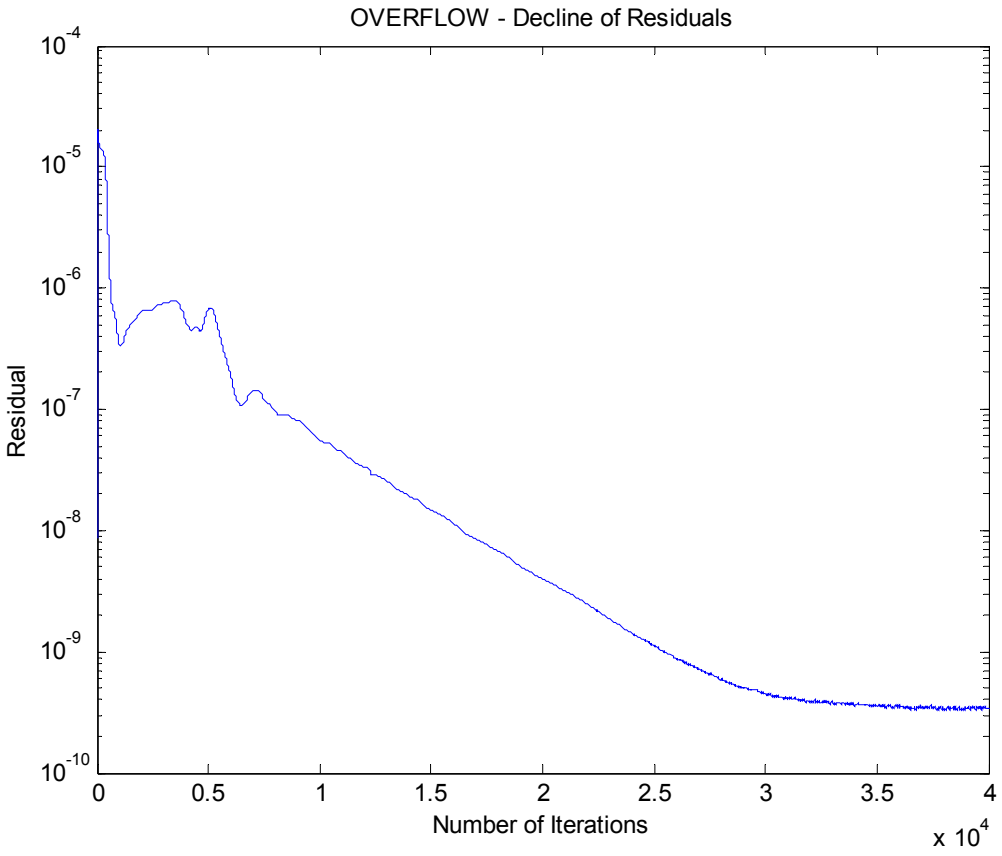

Figure 16. Residual decay as a function of iteration number.

It was seen from the figure that the solution converged after approx. 30,000 iterations. After this, the residuals had decayed by 4 or 5 orders of magnitude. This decay represented converged pressure gradients and boundary layers, demonstrating an accurate solution.

5. FAST

Flow Analysis Software Toolkit (FAST) developed by NASA Ames research center was used to compute and graphically represent the grid and its corresponding flow solution. Figure 17 shows a sample of such a representation showing the Mach number of the flow through the ramjet. Additional images are attached in Appendix I.

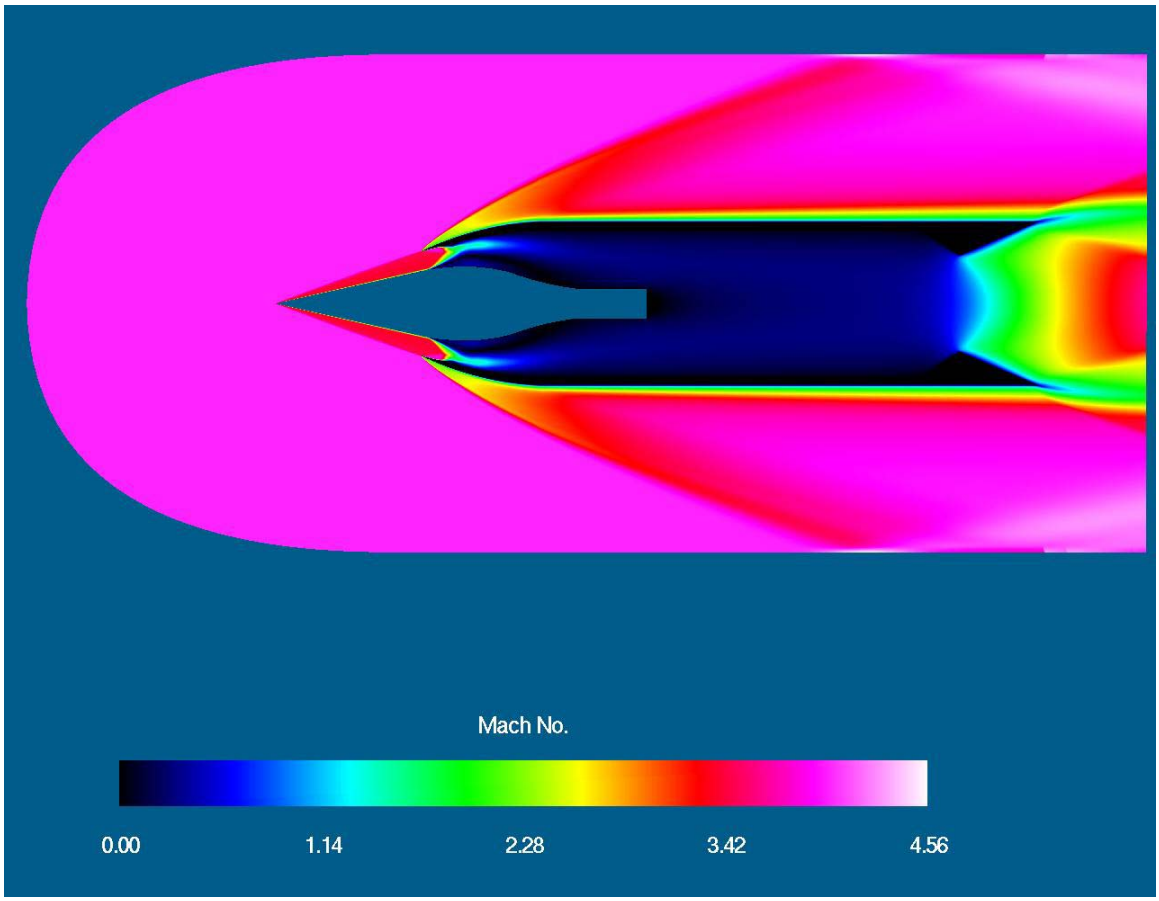

Figure 17. Viscous flow through ramjet at Mach 4.0 using FAST.

Many things were derived from this image, and images similar to it. The normal shock terminated on the cone in an oblique shock, which was formed by flow separation on the center body. Large regions of flow separation were evident downstream of the final shock. These regions were slightly reduced by recontouring the cowling inner profile, however they were not eliminated. The flow did decelerate to subsonic conditions through the inlet although the normal shock was not at the lip of the cowling. Finally, the gases leaving the nozzle were under expanded as the exhaust plume diverged aft of the nozzle.

THIS PAGE INTENTIONALLY LEFT BLANK

IV. FABRICATION

All parts were fabricated at the Mechanical Engineering machine shop at NPS. All parts to be exposed to heat were made of 304 stainless steel, including the combustion chamber and the nozzle. All other parts were made from 7075 aluminum alloy.

A. MACHINING

1. Cone

The ramjet cone is shown below in Figure 18. The cone was machined at an approximate 12-degree half angle with a total length of 1.4 inches.

Figure 18. Side view of ramjet cone with fuel injection ports at front.

The rear of the inlet cone contained a 7/16-24 UNS thread for easy attachment to the center body. The entire cone was machined hollow to allow fuel injection near the tip.

Aft of the inlet cone was the remainder of the center body and diffuser as shown in Figure 19. The center body was profiled for subsonic diffusion of the flow. The center body of the ramjet was also hollow (Figure 20) to allow fuel to flow between the struts and up to the tip of the cone.

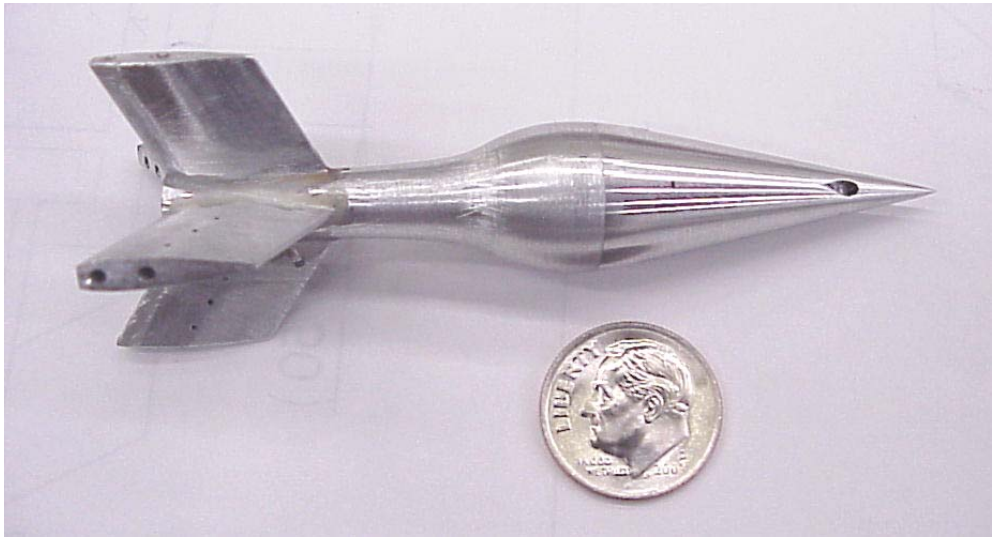

Figure 19. Machined and assembled ramjet center body.

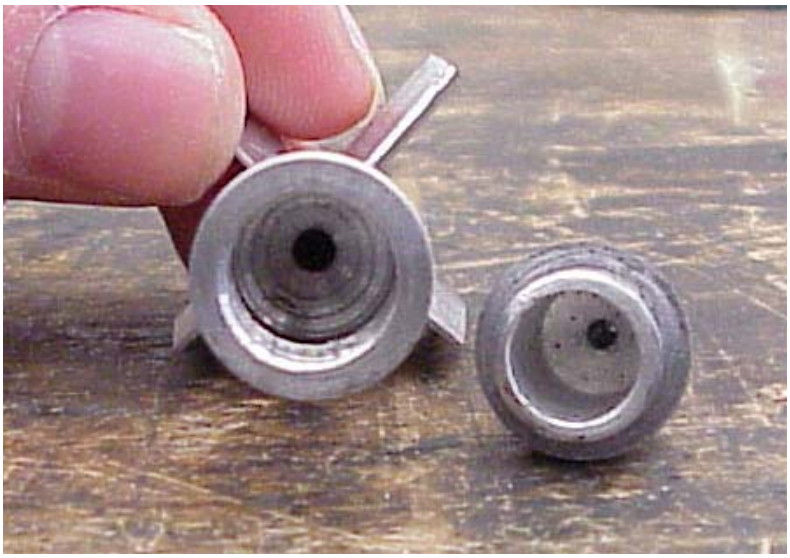

Figure 20. Disassembled inlet nose cone showing hollow interior and fuel passages.

2. Strut Assembly

The most intricate machining was done in the fuel injecting struts. These parts were to not only provide fuel to the engine, but were also to be used to position the cone relative to the lip of the intake. The assembly is shown in Figure 19 above and a detailed view is shown in Figure 21, which shows the rear fuel injection holes. These were tapped #0-80 and were closed with set screws until it would be determined experimentally if they were necessary for sustaining combustion or as attachment points for future flame holders.

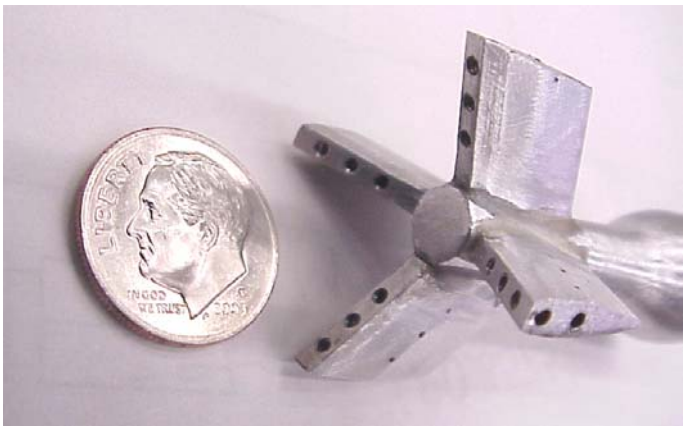

Figure 21. Detailed view of strut assembly with numerous fuel injection holes

3. Inlet Cowling

The inlet cowling of the ramjet is shown in Figure 22. It was made to be removable from the combustion chamber so that it could be remachined or replaced if the contour of this inlet had to be adjusted.

Figure 22. Inlet cowling of ramjet

3. Combustion Tube

The combustion section of the ramjet was machined from a 304 stainless steel tube to have all other parts attached to it. It was not a perfectly round cylinder as it had a welded seam in it, which created certain alignment problems.

Figure 23. Combustion chamber and body of ramjet.

4. Nozzle

The convergent-divergent nozzle of the ramjet was also machined out of 304 stainless steel stock. The nozzle was made removable so that additional nozzles could be machined and tested in the future if necessary.

Figure 24. Nozzle of ramjet.

B. ASSEMBLY

All parts were assembled using standard size machine screws and setscrews as well as Loctite® E-120HP Hysol® epoxy adhesive (Appendix F). The nozzle was screwed to the chamber for easy removal and replacement, if necessary. The intake was fastened to the combustion chamber using setscrews. The struts were attached to the center body using epoxy and locating pins. The strut and center body assembly was attached to the combustion chamber using screws. The final assembly is shown below in Figure 25. An exploded view of all the completed parts is shown in Figure 26. Also in this picture are the support struts used to hold the ramjet in the wind tunnel. They will be discussed in detail in the next chapter.

Figure 25. Assembled ramjet.

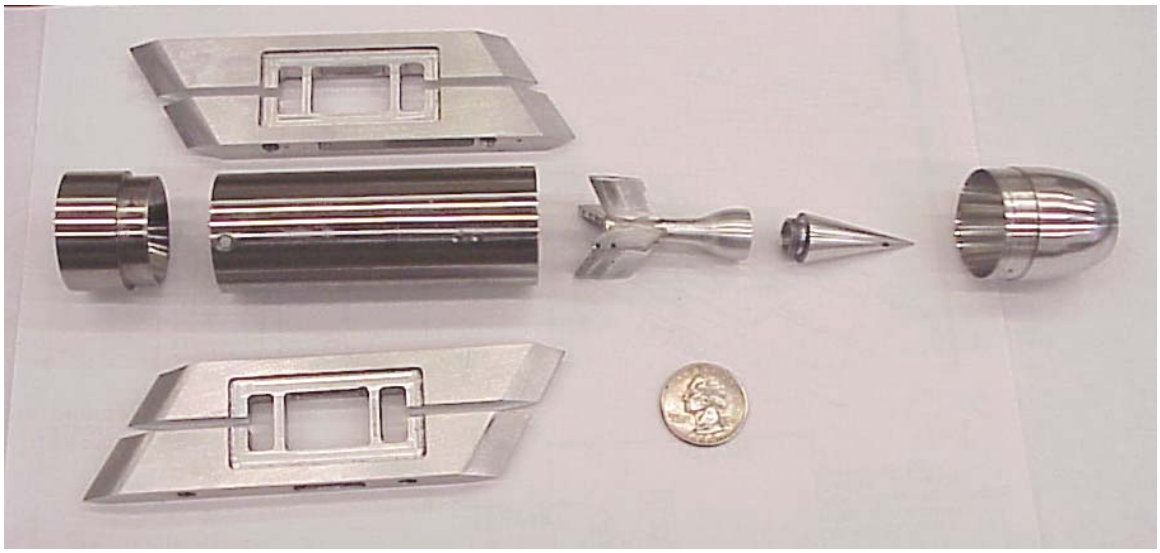

Figure 26. All manufactured parts of the ramjet including wind tunnel struts.

THIS PAGE INTENTIONALLY LEFT BLANK

V. WIND TUNNEL TESTING

A. WIND TUNNEL STRUTS

In order to hold the ramjet model in the wind tunnel test section, special struts were designed and built to measure the thrust and drag of the ramjet, and to allow fuel to be routed to the model. Figure 27 shows the strut alone. Figure 28 shows the strut with all other parts, and Figure 29 shows the parts within the wind tunnel. Figure 30 and Figure 31 show the assembled ramjet ready to be tested with the wind tunnel struts attached.

There were two flexure beams in the center of the strut which were to be instrumented with strain gauges to measure the thrust and drag of the ramjet. Strain gauges were not installed for the present study. Cover plates were fit on the top and bottom of this part to reduce drag and to protect the fuel lines and wiring to be contained within the part. Detailed part drawings of the struts and their cover plates are found in Appendix E.

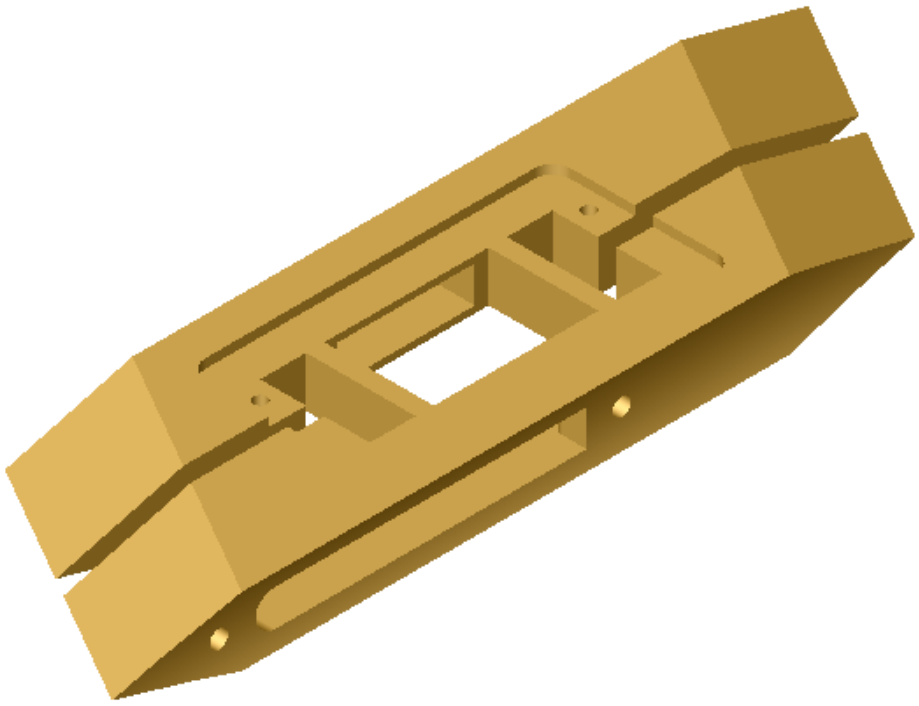

Figure 27. Isometric view of wind tunnel strut.

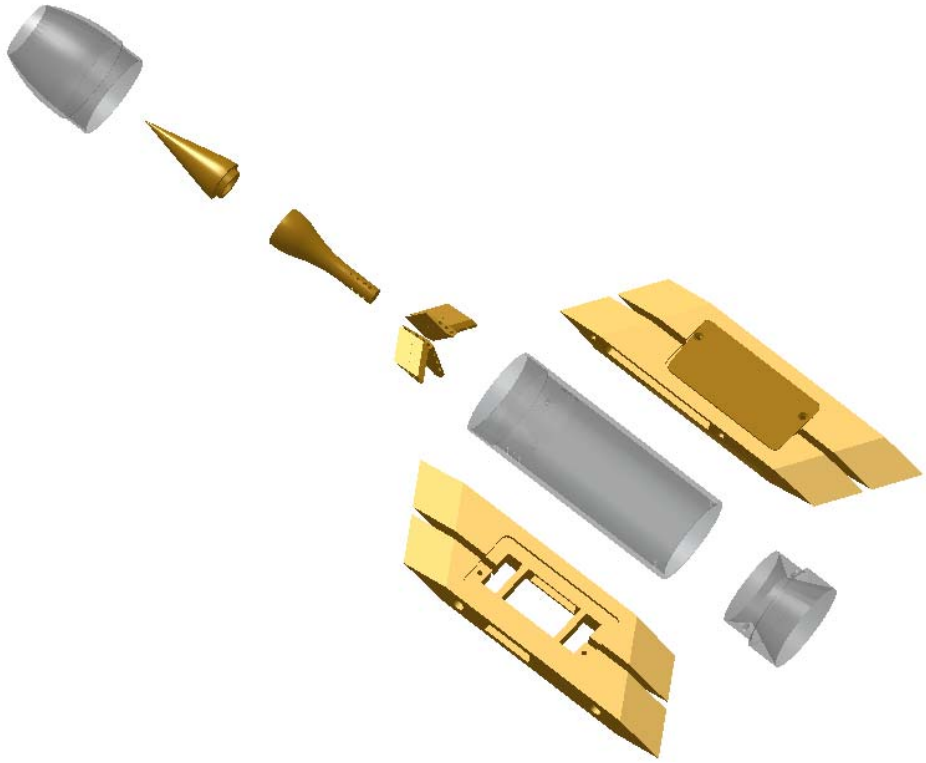

Figure 28. Exploded view of all parts of ramjet including wind tunnel support struts.

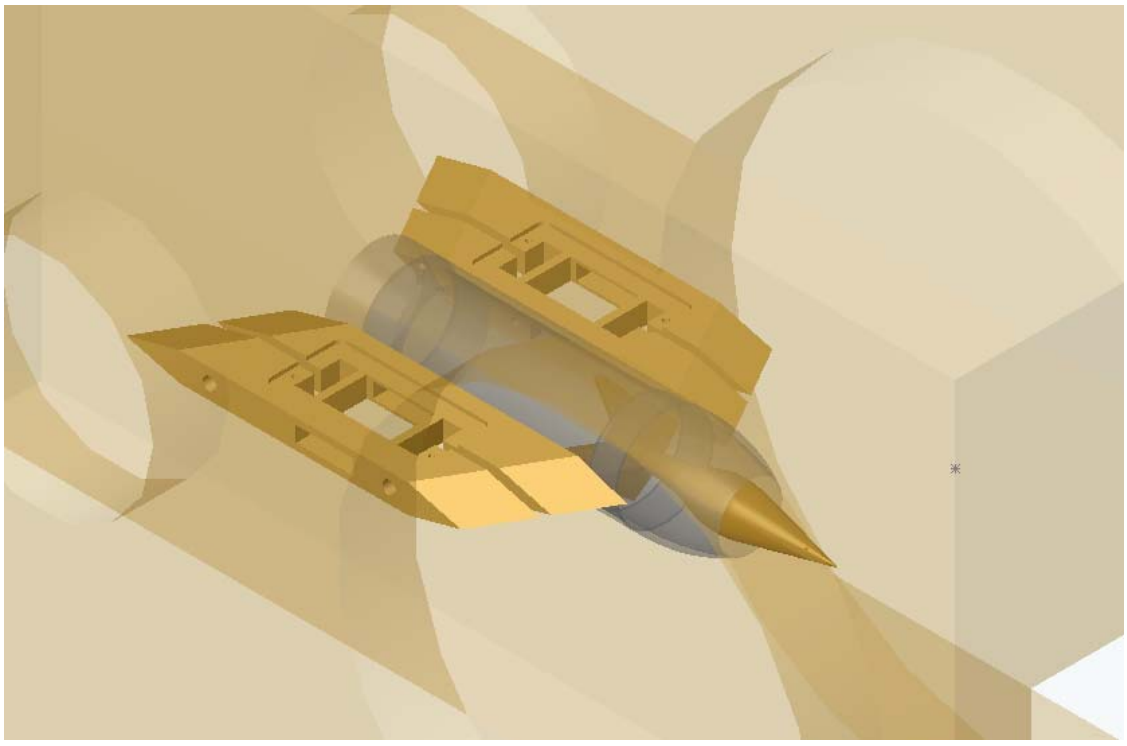

Figure 29. Detailed view of ramjet in wind tunnel with support struts.

The wind tunnel struts were attached to the body of the ramjet by pins near the front and by screws near the rear. Four attachment points were used to prevent the model from pitching up or down during testing.

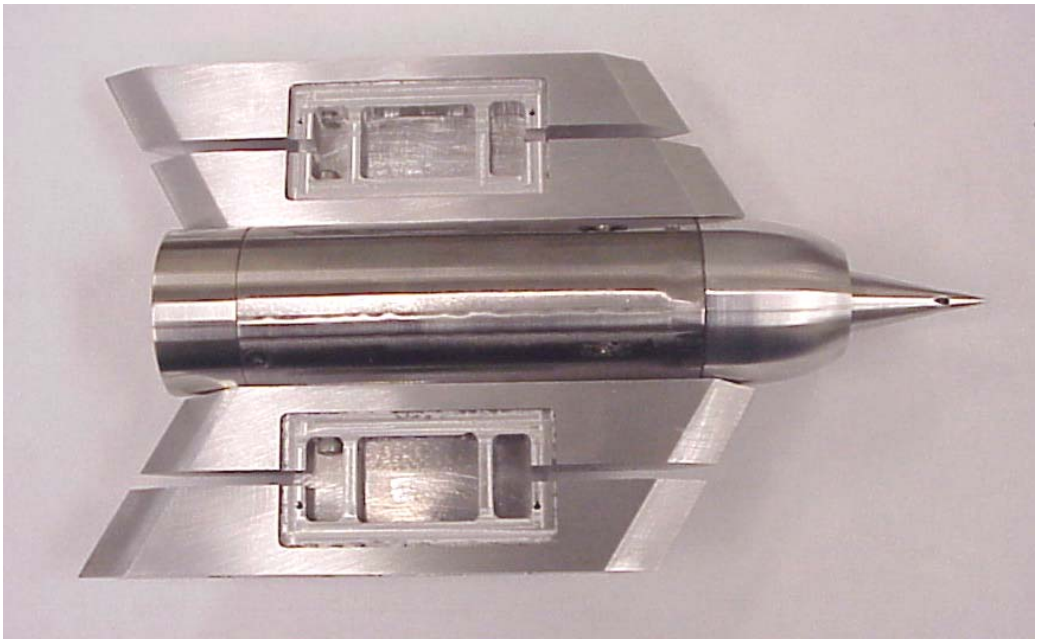

Figure 30. Assembled ramjet showing flexure beams.

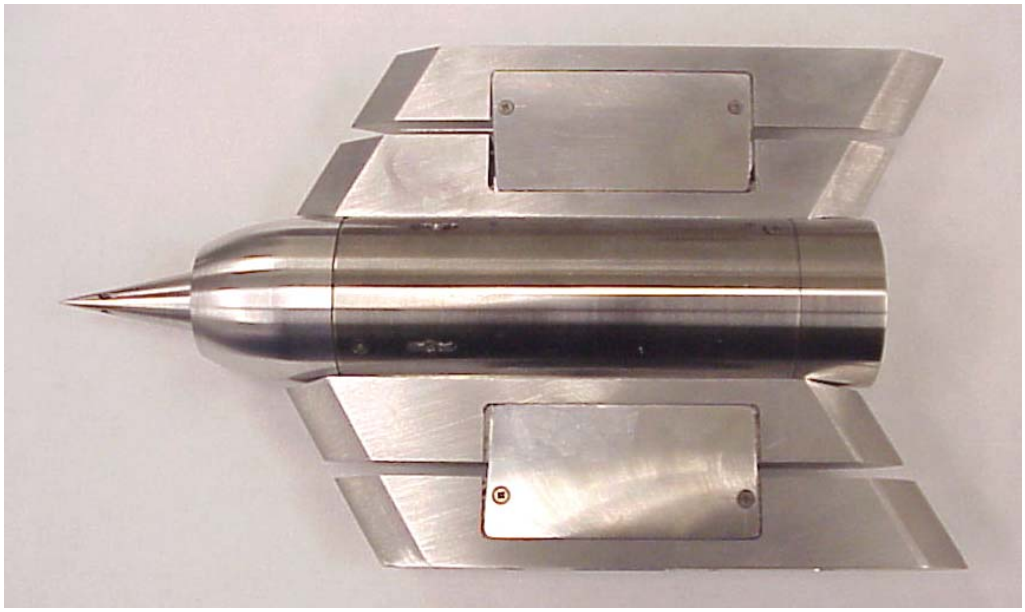

Figure 31. Assembled ramjet with cover plates prior to wind tunnel testing.

B. TESTING

The first wind tunnel test was run the afternoon of 9 June 2003. Prior to the test, the wind tunnel was run empty to blow out any accumulated debris or pipe scale, and to prevent damage to the model. The model was aligned parallel to the flow and then bolted to the wind tunnel. Figure 32 shows the ramjet mounted in the wind tunnel and ready to be tested.

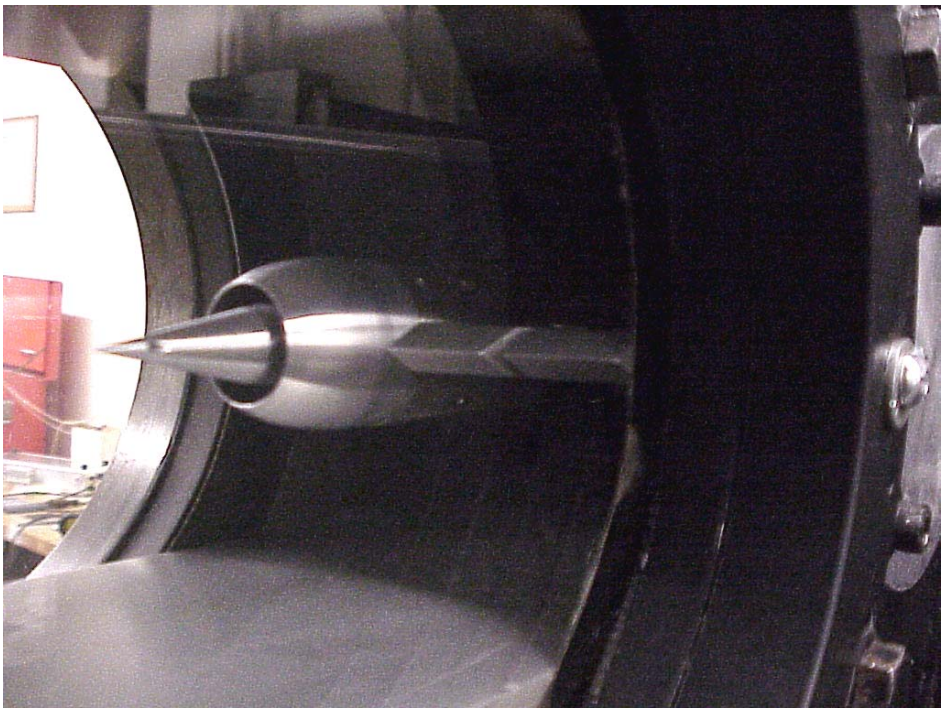

Figure 32. Photograph of ramjet in wind tunnel moments before testing.

The wind tunnel was brought up to speed. Throughout this transient period, the model underwent moments of large vibrations; but those vibrations disappeared once the starting shock moved over the model, and Mach 4 was established in the test section.

Video was taken throughout the testing period. A representative shadowgraph photo is shown in Figure 33. The oblique shock waves can be seen emanating from the tip of the cone and passing slightly over the intake. A slight misalignment can also be seen in this image as the oblique shock on the top of the image passes over the intake whereas the lower portion of the conical shock passes into the cowling. This shows a slight angle of attack of the model and therefore a small amount of misalignment.

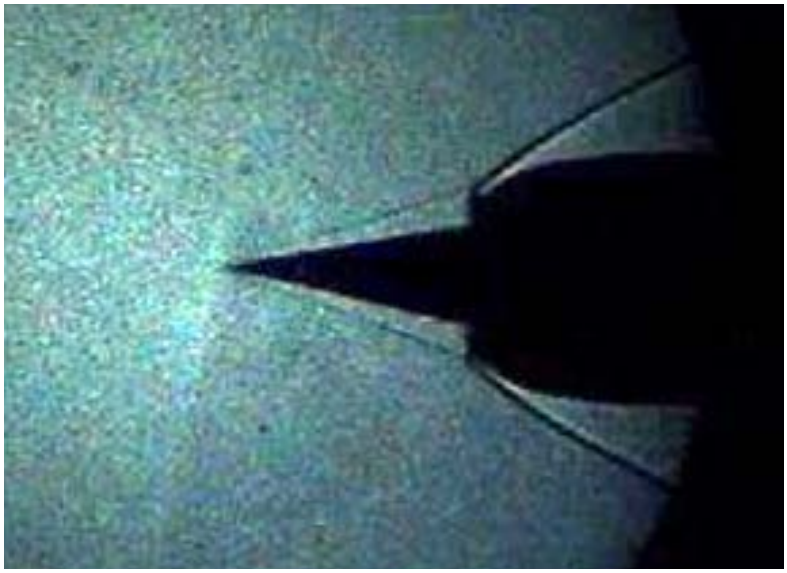

Figure 33. Shadowgraph image of ramjet in supersonic wind tunnel at Mach 4.0

The supersonic portion of the test ran successfully. The resulting oblique shock angles were 16.3 and 20.1 degrees. The discrepancy between the two angles showed the angle of attack of the ramjet to be approximately 2.1 degrees nose down. The average of these two angles being 18 degrees, whereas the shock angle for a 12.5 degree cone should be 19.6 degrees (see Appendix B). Due to an actual cone angle of slightly under 12 degrees the 18 degrees resulting was considered acceptable.

The tunnel was turned off after 2 minutes of testing. During this time, the inlet nose cone began to unscrew itself from the ramjet and eventually it unseated completely and was blown down the tunnel. The damaged cone is shown below in Figure 34.

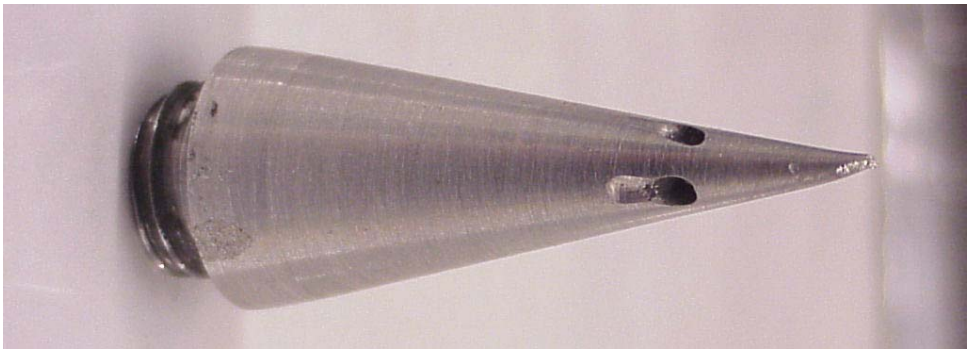

Figure 34. Inlet cone after being blown down the tunnel.

A second test run occurred on June 11, 2003 at 2:45 pm. Prior to the test, the inlet cone was repaired; secured into place using Loctite; and the model was returned to the wind tunnel. This test provided similar shadowgraph photos (Figure 35) as those in the first run. The oblique shocks were observed as in the first test run, although the ramjet's angle of attack was much closer to zero.

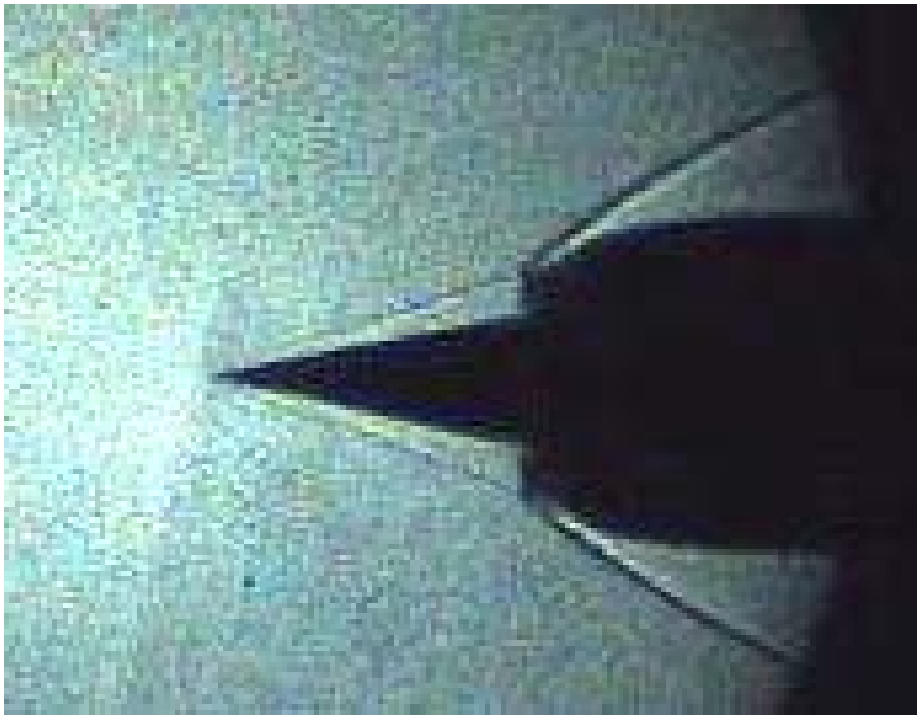

Figure 35. Shadowgraph of second test run at Mach 4.

An intermittent oblique shock structure on the cone of the model was observed on the video. This was thought to indicate the presence of a laminar boundary layer and normal shock interaction. Surface flow evidence for this is shown below in Figure 36.

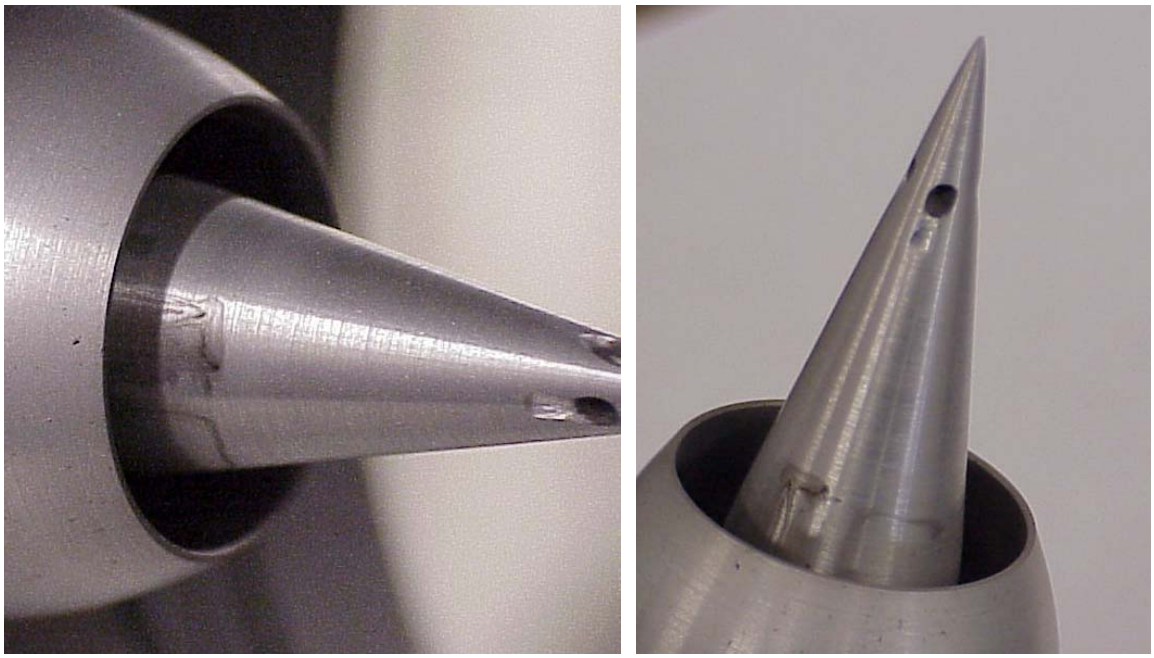

Figure 36. Post second run photographs of the inlet and residue remaining on the cone

Residue can be seen at the base of the inlet cone near the inlet. The residue occurred in the spaces that aligned with the gaps between the cone tip fuel ports. Air was ejecting out of the tip ports and then interacting with the normal shock. The injected air apparently eliminated what was most likely a laminar separation under a lambda shock structure.

THIS PAGE INTENTIONALLY LEFT BLANK

VI. CONCLUSIONS AND RECOMMENDATIONS

A wind tunnel model ramjet was successful designed, built and tested.

Several improvements in the fabrication and assembly of the ramjet could contribute to a more robust design and to obtaining more accurate data. These include:

- NC machine the center body and strut assembly to ensure proper alignment of fuel lines and mounting holes.
- Accurately machine the combustion tube to ensure axisymmetry.
- Use a finer thread on the inlet nose cone to prevent it from loosening during a wind tunnel test.

Additional work is needed to obtain drag and thrust data. Strain gauges should be added to the wind tunnel struts so that thrust and drag can be quantitatively measured. If necessary, the thickness of the wind tunnel strut flexure beams must be reduced so that they allow adequate sensitivity for the strain gauges.

More wind tunnel tests are necessary to fully evaluate the design. First, the reference drag must be measured by running the model in the tunnel with the strain gauges installed. Additionally, given the events from the second test run, it appears that the cone tip fuel injectors are beneficial to the inlet flow. Therefore, more holes should be added to the cone tip to cover the remaining areas of the intake that aren't yet affected by the tip injectors. This would restore the effective apparent intake area and allow the designed airflow through the ramjet. A detailed 3D CFD analysis of this interaction should also be undertaken to further understand what is taking place.

Finally, the thrust must be measured when the ramjet is ignited. Ignition of the burner may have to occur before running the wind tunnel and then remain sustained during starting of the tunnel. This challenging part of the ramjet development will have to be carried out on a trial and error basis.

THIS PAGE INTENTIONALLY LEFT BLANK

APPENDIX A. EXCEL CONE ANGLE SHOCK STUDY

Mach # Minf	Cone Angle Theta_s degrees	Oblique Shock Angle Theta_w rad	Oblique Shock Angle Theta_w deg	M1	M2 -- cone --	Pt2/Pt1	M1	M2 -- lip --	Pt2/Pt1	Ds/R	Pt1/Pinf	Pt2/Pt1 ave	**Pt2/Ptinf ave**
2													
	2.5	0.524	30.01	1.6243	0.6613	0.8860	1.6329	0.6588	0.8827	-1.118E-08	1.00000	0.88435	**0.884**
	5	0.525	30.09	1.6059	0.6667	0.8930	1.6311	0.6593	0.8834	1.118E-08	1.00000	0.88819	**0.888**
	7.5	0.531	30.45	1.5818	0.6740	0.9019	1.6238	0.6614	0.8862	3.104E-06	1.00000	0.89403	**0.894**
	10	0.545	31.21	1.5534	0.6830	0.9120	1.6084	0.6659	0.8920	5.746E-05	0.99994	0.90202	**0.902**
	12.5	0.565	32.38	1.5214	0.6936	0.9228	1.5848	0.6731	0.9008	4.704E-04	0.99953	0.91181	**0.911**
	15	0.592	33.91	1.4863	0.7060	0.9341	1.5545	0.6826	0.9116	1.624E-03	0.99838	0.92285	**0.921**
	17.5	0.624	35.74	1.4479	0.7204	0.9454	1.5188	0.6945	0.9237	4.524E-03	0.99549	0.93457	**0.930**
	20	0.660	37.80	1.4062	0.7371	0.9557	1.4786	0.7088	0.9364	9.963E-03	0.99009	0.94604	**0.937**
	22.5	0.699	40.07	1.3609	0.7568	0.9674	1.4343	0.7257	0.9492	1.867E-02	0.98151	0.95831	**0.941**
	25	0.742	42.53	1.3115	0.7802	0.9773	1.3858	0.7458	0.9617	3.117E-02	0.96931	0.9695	**0.940**
	27.5	0.789	45.20	1.2574	0.8085	0.9860	1.3329	0.7698	0.9732	4.781E-02	0.9533	0.97964	**0.934**
	30	0.839	48.08	1.1978	0.8435	0.9930	1.2750	0.7990	0.9835	6.881E-02	0.9335	0.98823	**0.923**
2.5													
	2.5	0.412	23.59	1.8169	0.6128	0.8052	1.8256	0.6109	0.8013	2.608E-08	1.0000	0.80321	**0.803**
	5	0.414	23.74	1.7989	0.6168	0.8132	1.8227	0.6115	0.8026	2.794E-07	1.0000	0.80787	**0.808**
	7.5	0.424	24.27	1.7756	0.6221	0.8235	1.8124	0.6138	0.8072	2.575E-05	1.0000	0.81531	**0.815**
	10	0.441	25.29	1.7484	0.6285	0.8353	1.7930	0.6181	0.8158	3.565E-04	0.9996	0.82552	**0.825**
	12.5	0.466	26.72	1.7180	0.6360	0.8482	1.7662	0.6242	0.8275	1.958E-03	0.9980	0.83787	**0.836**
	15	0.497	28.45	1.6844	0.6446	0.8621	1.7340	0.6320	0.8414	6.403E-03	0.9936	0.85177	**0.846**
	17.5	0.531	30.43	1.6477	0.6546	0.8769	1.6975	0.6412	0.8568	1.531E-02	0.9848	0.86683	**0.854**
	20	0.569	32.58	1.6075	0.6662	0.8924	1.6571	0.6520	0.8731	2.991E-02	0.9705	0.88276	**0.857**
	22.5	0.609	34.89	1.5636	0.6797	0.9084	1.6131	0.6645	0.8903	5.091E-02	0.9504	0.89934	**0.855**
	25	0.652	37.34	1.5157	0.6956	0.9247	1.5653	0.6792	0.9078	7.853E-02	0.9245	0.91628	**0.847**
	27.5	0.697	39.93	1.4635	0.7144	0.9409	1.5134	0.6964	0.9255	1.126E-01	0.8935	0.93321	**0.834**
	30	0.744	42.64	1.4064	0.7370	0.9566	1.4572	0.7168	0.9428	1.527E-01	0.8584	0.94967	**0.815**
3													
	2.5	0.340	19.49	1.9551	0.5852	0.7418	1.9637	0.5837	0.7408	3.353E-08	1.0000	0.74129	**0.741**
	5	0.344	19.72	1.9377	0.5885	0.7499	1.9596	0.5844	0.7397	2.183E-06	1.0000	0.74483	**0.745**
	7.5	0.357	20.46	1.9153	0.5927	0.7603	1.9465	0.5868	0.7458	1.339E-04	0.9999	0.75305	**0.753**
	10	0.379	21.71	1.8894	0.5977	0.7722	1.9247	0.5909	0.7559	1.401E-03	0.9986	0.76409	**0.763**
	12.5	0.408	23.35	1.8603	0.6036	0.7856	1.8967	0.5963	0.7689	6.231E-03	0.9938	0.77722	**0.772**
	15	0.441	25.26	1.8279	0.6104	0.8002	1.8641	0.6028	0.7838	1.749E-02	0.9827	0.792	**0.778**
	17.5	0.478	27.36	1.7921	0.6183	0.8162	1.8278	0.6106	0.8001	3.736E-02	0.9633	0.80816	**0.779**
	20	0.517	29.61	1.7526	0.6275	0.8335	1.7877	0.6193	0.8181	6.695E-02	0.9352	0.82579	**0.772**
	22.5	0.558	32.00	1.7090	0.6382	0.8520	1.7439	0.6296	0.8372	1.064E-01	0.8990	0.84458	**0.759**
	25	0.608	34.83	1.6612	0.6509	0.8715	1.6961	0.6415	0.8573	1.552E-01	0.8562	0.86442	**0.740**
	27.5	0.647	37.09	1.6089	0.6658	0.8918	1.6442	0.6556	0.8783	2.124E-01	0.8086	0.88505	**0.716**
	30	0.694	39.78	1.5519	0.6835	0.9125	1.5879	0.6721	0.8997	2.767E-01	0.7583	0.9061	**0.687**
3.5													
	2.5	0.290	16.63	2.0555	0.5682	0.6949	2.0638	0.5669	0.6911	-2.608E-08	1.0000	0.693	**0.693**
	5	0.296	16.95	2.0387	0.5709	0.7028	2.0584	0.5677	0.6936	1.098E-05	1.0000	0.69819	**0.698**
	7.5	0.312	17.90	2.0173	0.5744	0.7128	2.0433	0.5701	0.7007	4.856E-04	0.9995	0.70671	**0.706**
	10	0.338	19.36	1.9926	0.5786	0.7243	2.0203	0.5739	0.7114	3.975E-03	0.9960	0.71786	**0.715**
	12.5	0.369	21.16	1.9646	0.5836	0.7374	1.9922	0.5787	0.7245	1.496E-02	0.9851	0.73098	**0.720**
	15	0.405	23.20	1.9330	0.5893	0.7521	1.9600	0.5844	0.7395	3.739E-02	0.9633	0.74581	**0.718**
	17.5	0.443	25.41	1.8978	0.5961	0.7684	1.9241	0.5910	0.7562	7.337E-02	0.9293	0.76231	**0.708**
	20	0.484	27.74	1.8585	0.6039	0.7864	1.8843	0.5987	0.7746	1.232E-01	0.8841	0.78048	**0.690**
	22.5	0.527	30.19	1.8149	0.6132	0.8060	1.8406	0.6077	0.7945	1.861E-01	0.8302	0.80026	**0.664**
	25	0.571	32.73	1.7668	0.6241	0.8273	1.7928	0.6181	0.8159	2.602E-01	0.7709	0.82158	**0.633**
	27.5	0.617	35.35	1.7141	0.6369	0.8498	1.7405	0.6304	0.8386	3.438E-01	0.7091	0.84424	**0.599**
	30	0.664	38.06	1.6565	0.6522	0.8734	1.6837	0.6448	0.8624	4.347E-01	0.6475	0.86792	**0.562**
4													
	2.5	0.253	14.51	2.1296	0.5569	0.6605	2.1376	0.5557	0.6568	3.737E-08	1.0000	0.65863	**0.659**
	5	0.261	14.96	2.1135	0.5583	0.6587	2.1309	0.5567	0.6599	4.119E-05	1.0000	0.65927	**0.659**
	7.5	0.281	16.09	2.0931	0.5619	0.6774	2.1145	0.5578	0.6582	1.347E-03	0.9987	0.66782	**0.667**
	10	0.309	17.71	2.0694	0.5660	0.6885	2.0912	0.5626	0.6783	8.993E-03	0.9910	0.68337	**0.677**
	12.5	0.343	19.65	2.0422	0.5703	0.7012	2.0635	0.5669	0.6912	2.967E-02	0.9708	0.69619	**0.676**
	15	0.380	21.79	2.0113	0.5754	0.7156	2.0318	0.5720	0.7060	6.773E-02	0.9345	0.7108	**0.664**
	17.5	0.420	24.08	1.9763	0.5815	0.7319	1.9883	0.5794	0.7264	1.244E-01	0.8830	0.72914	**0.644**
	20	0.462	26.49	1.9371	0.5886	0.7502	1.9568	0.5849	0.7410	1.987E-01	0.8198	0.74561	**0.611**
	22.5	0.506	28.98	1.8933	0.5969	0.7606	1.9131	0.5931	0.7613	2.881E-01	0.7497	0.76093	**0.570**
	25	0.551	31.56	1.8449	0.6068	0.7926	1.8650	0.6026	0.7834	3.899E-01	0.6771	0.78797	**0.534**
	27.5	0.597	34.21	1.7916	0.6184	0.8164	1.8124	0.6138	0.8072	5.011E-01	0.6059	0.81178	**0.492**
	30	0.645	36.94	1.7333	0.6321	0.8417	1.7550	0.6269	0.8324	6.189E-01	0.5386	0.83705	**0.451**

Figure 37. Calculation to determine optimal recovery ratio for different Mach numbers.

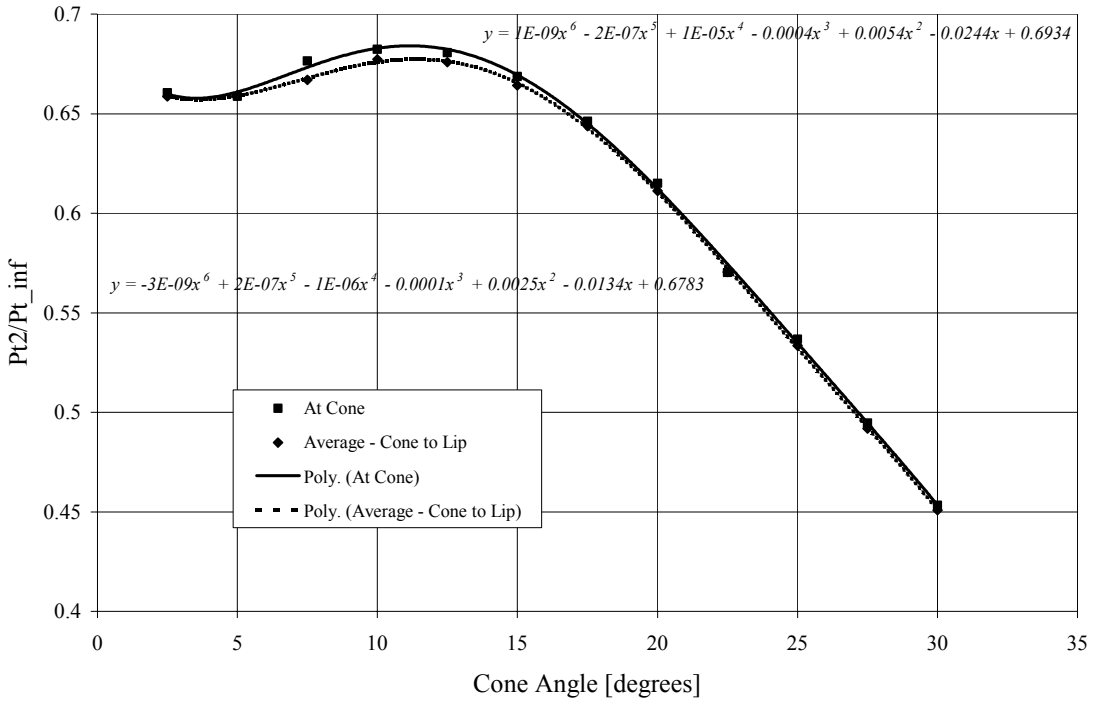

Figure 38. Normal shock recovery pressure ratio vs. cone angle at cone and lip of inlet cowling at Mach 4.0

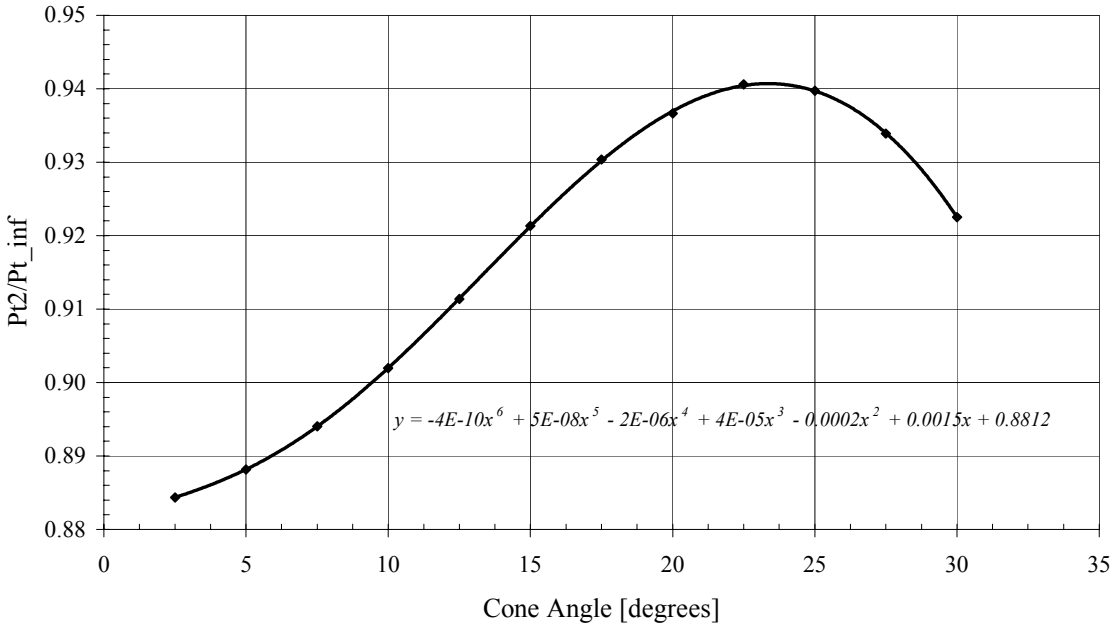

Figure 39. Normal shock recovery pressure ratio vs. cone angle at Mach 2.0

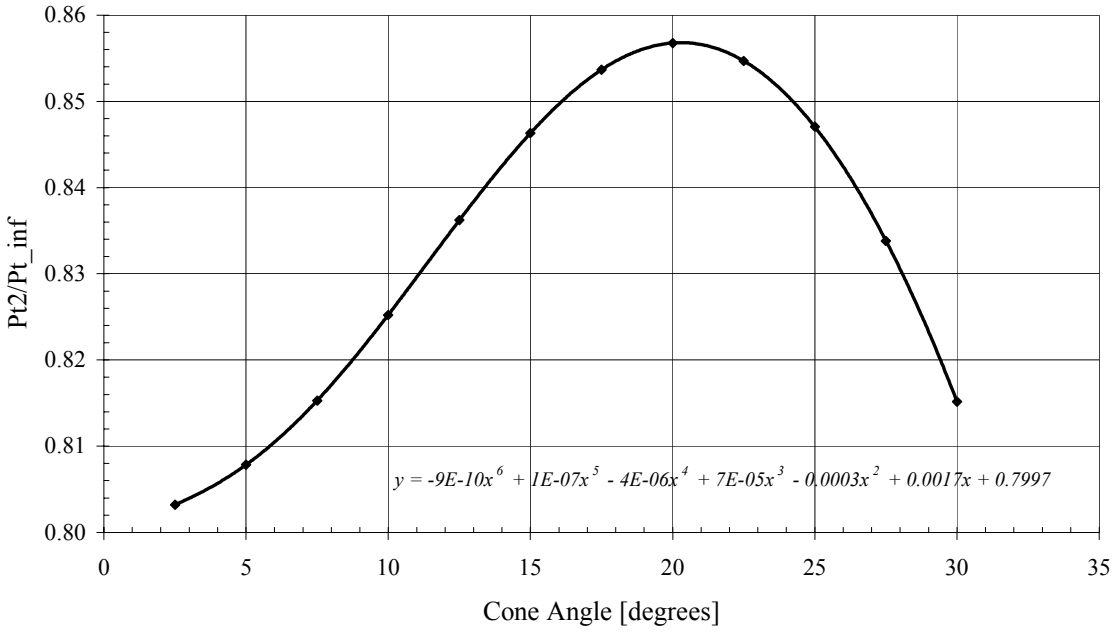

Figure 40. Normal shock recovery pressure ratio vs. cone angle at Mach 2.5

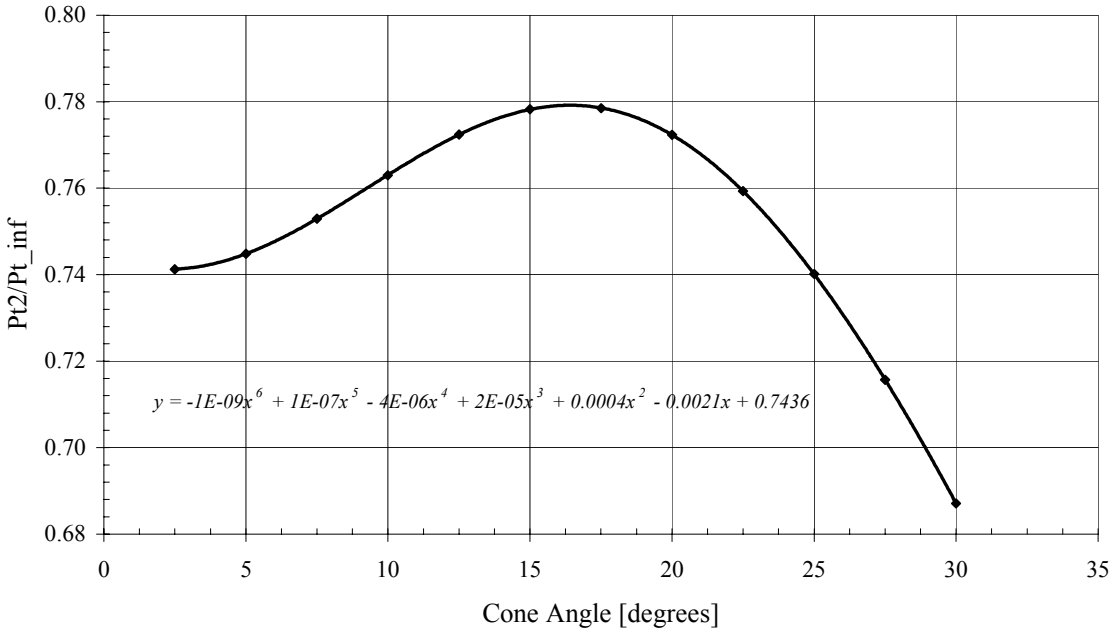

Figure 41. Normal shock recovery pressure ratio vs. cone angle at Mach 3.0

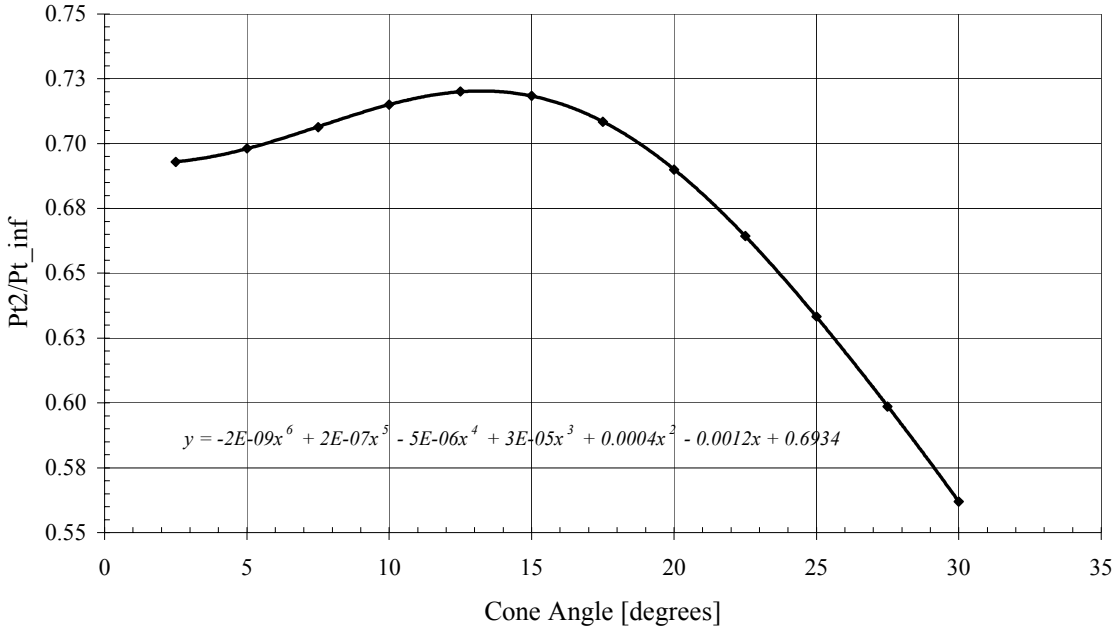

Figure 42. Normal shock recovery pressure ratio vs. cone angle at Mach 3.5

APPENDIX B. SAMPLE SHOCK CALCULATION

$M_\infty = 4.0$

$\theta_s = 10°$ (cone angle)

$\theta_w = 17.71°$ (oblique shock angle)

use conic shock tables [ref. 1] to determine Mach numbers at cone and at lip

at cone: $M1^* = 2.042$

use normal shock tables [ref. 2];

$M2 = 0.566, \;\; Pt2/Pt1 = 0.6885$

at lip: $M1^* = 2.0912$

use normal shock table;

$M2 = 0.562, \;\; Pt2/Pt1 = 0.6783$

Also:

$\Delta s/R = .00899 = \ln(Pt1/Pt_\infty)$

hence, $Pt1/Pt_\infty = 0.991$

Finally:

$(Pt2/Pt1)_{average} = 0.683$

$\therefore (Pt2/Pt_\infty)_{average} = (Pt1/Pt_\infty)(Pt2/Pt1)_{average} = 0.677$

THIS PAGE INTENTIONALLY LEFT BLANK

APPENDIX C. EXCEL AREA CALCULATIONS

M6	A6	Cone Angle (alpha)		Shock Angle (beta)		M1	M2	A6/A6*	A2/A2*	A6/A2	A2
		Deg	Rad	Deg	Rad	-cone-					
0.3	1.1028757	10	0.1745	17.71484	0.3091822	2.069365	0.56599	2.03507	1.2319274	0.6053489	0.6676246
		11	0.1920	18.48889	0.3226921	2.058496	0.567724	2.03507	1.2295071	0.6041596	0.6663129
		12	0.2094	19.26295	0.336202	2.047627	0.569458	2.03507	1.2270867	0.6029703	0.6650013
	0.9451552	10	0.1745	17.71484	0.3091822	2.069365	0.56599	2.03507	1.2319274	0.6053489	0.5721487
		11	0.1920	18.48889	0.3226921	2.058496	0.567724	2.03507	1.2295071	0.6041596	0.5710246
		12	0.2094	19.26295	0.336202	2.047627	0.569458	2.03507	1.2270867	0.6029703	0.5699005
	0.8642529	10	0.1745	17.71484	0.3091822	2.069365	0.56599	2.03507	1.2319274	0.6053489	0.5231746
		11	0.1920	18.48889	0.3226921	2.058496	0.567724	2.03507	1.2295071	0.6041596	0.5221467
		12	0.2094	19.26295	0.336202	2.047627	0.569458	2.03507	1.2270867	0.6029703	0.5211188
0.25	1.1028757	10	0.1745	17.71484	0.3091822	2.069365	0.56599	2.040271	1.2319274	0.6038058	0.6659227
		11	0.1920	18.48889	0.3226921	2.058496	0.567724	2.040271	1.2295071	0.6026195	0.6646144
		12	0.2094	19.26295	0.336202	2.047627	0.569458	2.040271	1.2270867	0.6014332	0.6633061
	0.9451552	10	0.1745	17.71484	0.3091822	2.069365	0.56599	2.040271	1.2319274	0.6038058	0.5706902
		11	0.1920	18.48889	0.3226921	2.058496	0.567724	2.040271	1.2295071	0.6026195	0.5695689
		12	0.2094	19.26295	0.336202	2.047627	0.569458	2.040271	1.2270867	0.6014332	0.5684477
	0.8642529	10	0.1745	17.71484	0.3091822	2.069365	0.56599	2.040271	1.2319274	0.6038058	0.5218409
		11	0.1920	18.48889	0.3226921	2.058496	0.567724	2.040271	1.2295071	0.6026195	0.5208156
		12	0.2094	19.26295	0.336202	2.047627	0.569458	2.040271	1.2270867	0.6014332	0.5197904
0.2	1.1028757	10	0.1745	17.71484	0.3091822	2.069365	0.56599	2.96352	1.2319274	0.4156974	0.4584625
		11	0.1920	18.48889	0.3226921	2.058496	0.567724	2.96352	1.2295071	0.4148806	0.4575618
		12	0.2094	19.26295	0.336202	2.047627	0.569458	2.96352	1.2270867	0.4140639	0.456661
	0.9451552	10	0.1745	17.71484	0.3091822	2.069365	0.56599	2.96352	1.2319274	0.4156974	0.3928985
		11	0.1920	18.48889	0.3226921	2.058496	0.567724	2.96352	1.2295071	0.4148806	0.3921266
		12	0.2094	19.26295	0.336202	2.047627	0.569458	2.96352	1.2270867	0.4140639	0.3913547
	0.8642529	10	0.1745	17.71484	0.3091822	2.069365	0.56599	2.96352	1.2319274	0.4156974	0.3592677
		11	0.1920	18.48889	0.3226921	2.058496	0.567724	2.96352	1.2295071	0.4148806	0.3585618
		12	0.2094	19.26295	0.336202	2.047627	0.569458	2.96352	1.2270867	0.4140639	0.3578559
0.15	1.05883	10	0.1745	17.71484	0.3091822	2.069365	0.56599	3.91034	1.2319274	0.3150436	0.3335776
		11	0.1920	18.48889	0.3226921	2.058496	0.567724	3.91034	1.2295071	0.3144246	0.3329222
		12	0.2094	19.26295	0.336202	2.047627	0.569458	3.91034	1.2270867	0.3138056	0.3322668
	0.9451552	10	0.1745	17.71484	0.3091822	2.069365	0.56599	3.91034	1.2319274	0.3150436	0.2977651
		11	0.1920	18.48889	0.3226921	2.058496	0.567724	3.91034	1.2295071	0.3144246	0.29718
		12	0.2094	19.26295	0.336202	2.047627	0.569458	3.91034	1.2270867	0.3138056	0.296595
	0.8642529	10	0.1745	17.71484	0.3091822	2.069365	0.56599	3.91034	1.2319274	0.3150436	0.2722773
		11	0.1920	18.48889	0.3226921	2.058496	0.567724	3.91034	1.2295071	0.3144246	0.2717424
		12	0.2094	19.26295	0.336202	2.047627	0.569458	3.91034	1.2270867	0.3138056	0.2712074

Figure 43. Preliminary calculations to determine necessary intake area.

THIS PAGE INTENTIONALLY LEFT BLANK

APPENDIX D. GASTURB FILES

Methane

Station	W	T	P	WRstd						
amb		389.97	1.088		FN	=	32.02	Altitude	ft	59055.12
1		1588.4	171.072		SFC	=	1.9709	Delta T from ISA	R	0
2	0.424	1588.4	113.592	0.096	WF	=	0.01753	Relative Humidity [%]		0
61	0.407	1588.4	110.184		FN/W2	=	2432.0296	Mach Number		4
7	0.424	4320.00	106.754		P2/P1	=	0.6640	Inlet Corr. Flow W2Rstd	lb/s	0.0959139
8	0.441	4218.7	106.754		A8	=	0.5229	Intake Pressure Ratio P2/P1		0.664
Burner Efficiency			0.9500		P8/Pamb	=	98.0755	Diffuser Pressure Ratio P6/P2		0.97
Jetpipe Diam.			1.1850		A61	=	1.10288	Burner Exit Temperature	R	4320
Pressure Loss [%]			3.11		XM6	=	0.15000	Burner Efficiency		0.95
Con-Di Nozzle:					XM7	=	0.28392	Fuel Heating Value	BTU/lb	23231.36
A9*(Ps9-Pamb)			8.933		A9/A8	=	2.59754	Nozzle Cooling Air Wcl/W6		0.04
					XM9	=	2.34822	Burner Inlet Mach Number		0.15
					CFGid	=	0.93320	Nozzle Thrust Coefficient		1
								Con-Di Nozzle:		
								Nozzle Area Ratio		2.5972

Propane

Station	W	T	P	WRstd						
amb		389.97	1.088		FN	=	32.34	Altitude	ft	59055.12
1		1588.4	171.072		SFC	=	2.1213	Delta T from ISA	R	0
2	0.424	1588.4	113.592	0.096	WF	=	0.01906	Relative Humidity [%]		0
61	0.407	1588.4	110.184		FN/W2	=	2456.1503	Mach Number		4
7	0.426	4320.00	106.714		P2/P1	=	0.6640	Inlet Corr. Flow W2Rstd	lb/s	0.0959139
8	0.443	4218.98	106.714		A8	=	0.5253	Intake Pressure Ratio P2/P1		0.664
Burner Efficiency			0.9500		P8/Pamb	=	98.0393	Diffuser Pressure Ratio P6/P2		0.97
Jetpipe Diam.			1.1850		A61	=	1.10288	Burner Exit Temperature	R	4320
Pressure Loss [%]			3.15		XM6	=	0.15000	Burner Efficiency		0.95
Con-Di Nozzle:					XM7	=	0.28545	Fuel Heating Value	BTU/lb	21669
A9*(Ps9-Pamb)			9.04		A9/A8	=	2.58561	Nozzle Cooling Air Wcl/W6		0.04
					XM9	=	2.34196	Burner Inlet Mach Number		0.15
					CFGid	=	0.93225	Nozzle Thrust Coefficient		1
								Con-Di Nozzle:		
								Nozzle Area Ratio		2.5856

Hydrogen

Station	W	T	P	WRstd						
amb		389.97	1.088		FN	=	29.53	Altitude	ft	59055.12
1		1588.4	171.072		SFC	=	0.7006	Delta T from ISA	R	0
2	0.424	1588.4	113.592	0.096	WF	=	0.00575	Relative Humidity [%]		0
61	0.407	1588.4	110.184		FN/W2	=	2242.9935	Mach Number		4
7	0.412	4320.00	107.052		P2/P1	=	0.6640	Inlet Corr. Flow W2Rstd	lb/s	0.0959139
8	0.429	4216.51	107.052		A8	=	0.5047	Intake Pressure Ratio P2/P1		0.664
Burner Efficiency			0.9500		P8/Pamb	=	98.3498	Diffuser Pressure Ratio P6/P2		0.97
Jetpipe Diam.			1.1850		A6	=	1.10288	Burner Exit Temperature	R	4320
Pressure Loss [%]			2.84		XM6	=	0.15000	Burner Efficiency		0.95
Con-Di Nozzle:					XM7	=	0.27230	Fuel Heating Value	BTU/lb	61095
A9*(Ps9-Pamb)			8.102		A9/A8	=	2.69078	Nozzle Cooling Air Wcl/W6		0.04
					XM9	=	2.40086	Burner Inlet Mach Number		0.15
					CFGid	=	0.94055	Nozzle Thrust Coefficient		1
								Con-Di Nozzle:		
								Nozzle Area Ratio		2.6908

Table 4. GASTURB data showing change in SFC for different fuels.

Kerosene

Station	W	T	P	WRstd	FN	=	32.76	Altitude	ft	59055.12
amb		389.97	1.088		SFC	=	2.3151	Delta T from ISA	R	0
1		1588.4	171.072		WF	=	2.107E-02	Relative Humidity [%]		0
2	0.424	1588.4	113.592	0.096	FN/W2	=	2487.8002	Mach Number		4
61	0.407	1588.4	110.184		P2/P1	=	0.6640	Inlet Corr. Flow W2Rstd	lb/s	0.0959139
7	0.428	4320.00	106.754		A8	=	0.5284	Intake Pressure Ratio P2/P1		0.664
8	0.445	4219.35	106.754		P8/Pamb	=	97.9913	Diffuser Pressure Ratio P6/P2		0.97
Burner Efficiency			0.9500		A6	=	1.10288	Burner Exit Temperature	R	4320
Jetpipe Diam.			1.1850		XM6	=	0.15000	Burner Efficiency		0.95
Pressure Loss [%]			3.20		XM7	=	0.28748	Fuel Heating Value	BTU/lb	19940
Con-Di Nozzle:					A9/A8	=	2.57045	Nozzle Cooling Air Wcl/W6		0.04
A9*(Ps9-Pamb)			9.182		XM9	=	2.33387	Burner Inlet Mach Number		0.15
					CFGid	=	0.93101	Nozzle Thrust Coefficient		1
								Con-Di Nozzle:		
								Nozzle Area Ratio		2.5705

JP-10

Station	W	T	P	WRstd	FN	=	33.28	Altitude	ft	59055.12
amb		389.97	1.088		SFC	=	2.5527	Delta T from ISA	R	0
1		1588.4	171.072		WF	=	2.360E-02	Relative Humidity [%]		0
2	0.424	1588.4	113.592	0.096	FN/W2	=	2527.531	Mach Number		4
61	0.407	1588.4	110.184		P2/P1	=	0.6640	Inlet Corr. Flow W2Rstd	lb/s	0.0959139
7	0.43	4320.00	106.596		A8	=	0.5323	Intake Pressure Ratio P2/P1		0.664
8	0.447	4219.81	106.596		P8/Pamb	=	97.9303	Diffuser Pressure Ratio P6/P2		0.97
Burner Efficiency			0.9500		A6	=	1.10288	Burner Exit Temperature	R	4320
Jetpipe Diam.			1.1850		XM6	=	0.15000	Burner Efficiency		0.95
Pressure Loss [%]			3.26		XM7	=	0.29005	Fuel Heating Value	BTU/lb	18137
Con-Di Nozzle:					A9/A8	=	2.55158	Nozzle Cooling Air Wcl/W6		0.04
A9*(Ps9-Pamb)			9.361		XM9	=	2.32391	Burner Inlet Mach Number		0.15
					CFGid	=	0.92944	Nozzle Thrust Coefficient		1
								Con-Di Nozzle:		
								Nozzle Area Ratio		2.5516

Table 4 (cont'd). GASTURB data showing change in SFC for different fuels.

Fuel Type	*Heating Value* [BTU/lb]	*Specific Fuel Consumption*
Hydrogen	61095	0.7006
Methane	23231	1.9709
Propane	21669	2.1213
Kerosene	19940	2.3151
JP-10	18137	2.5527

Table 5. Summary of GASTURB fuel efficiencies from Table 4.

APPENDIX E. DETAILED PART DRAWINGS

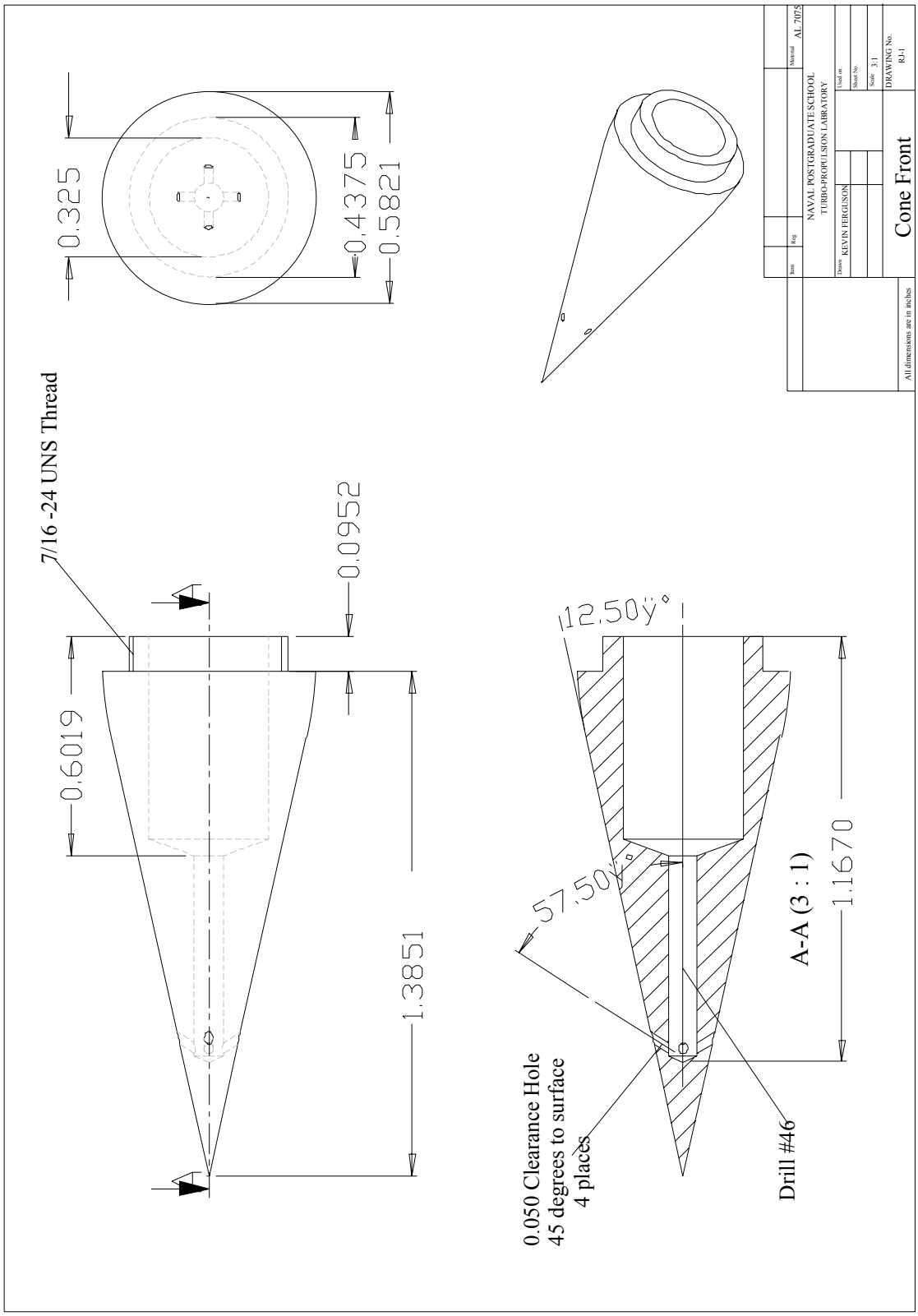

Figure 44. Part drawing: Ramjet inlet nose cone (RJ-1)

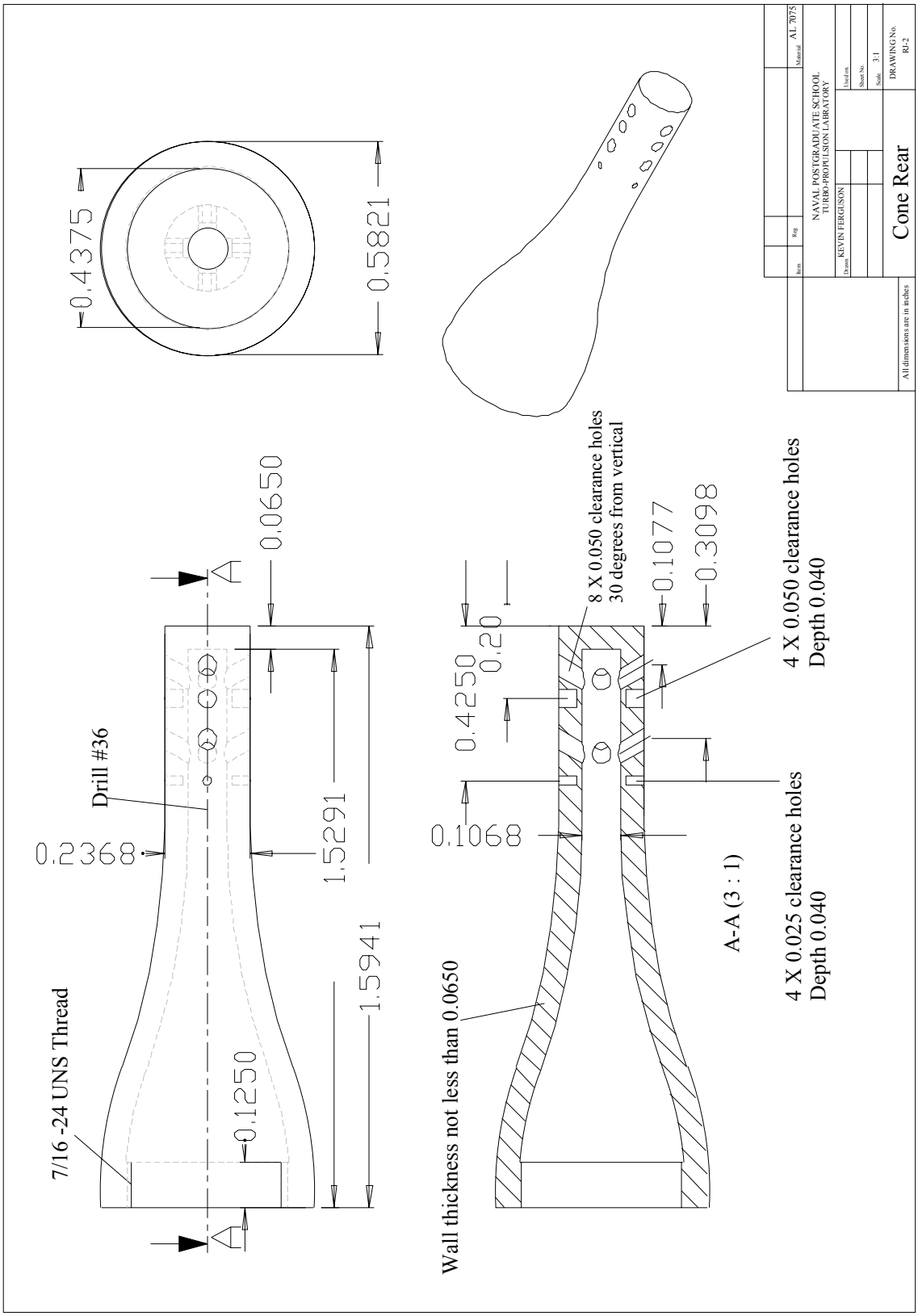

Figure 45. Part drawing: Rear of inlet nose cone (RJ-2)

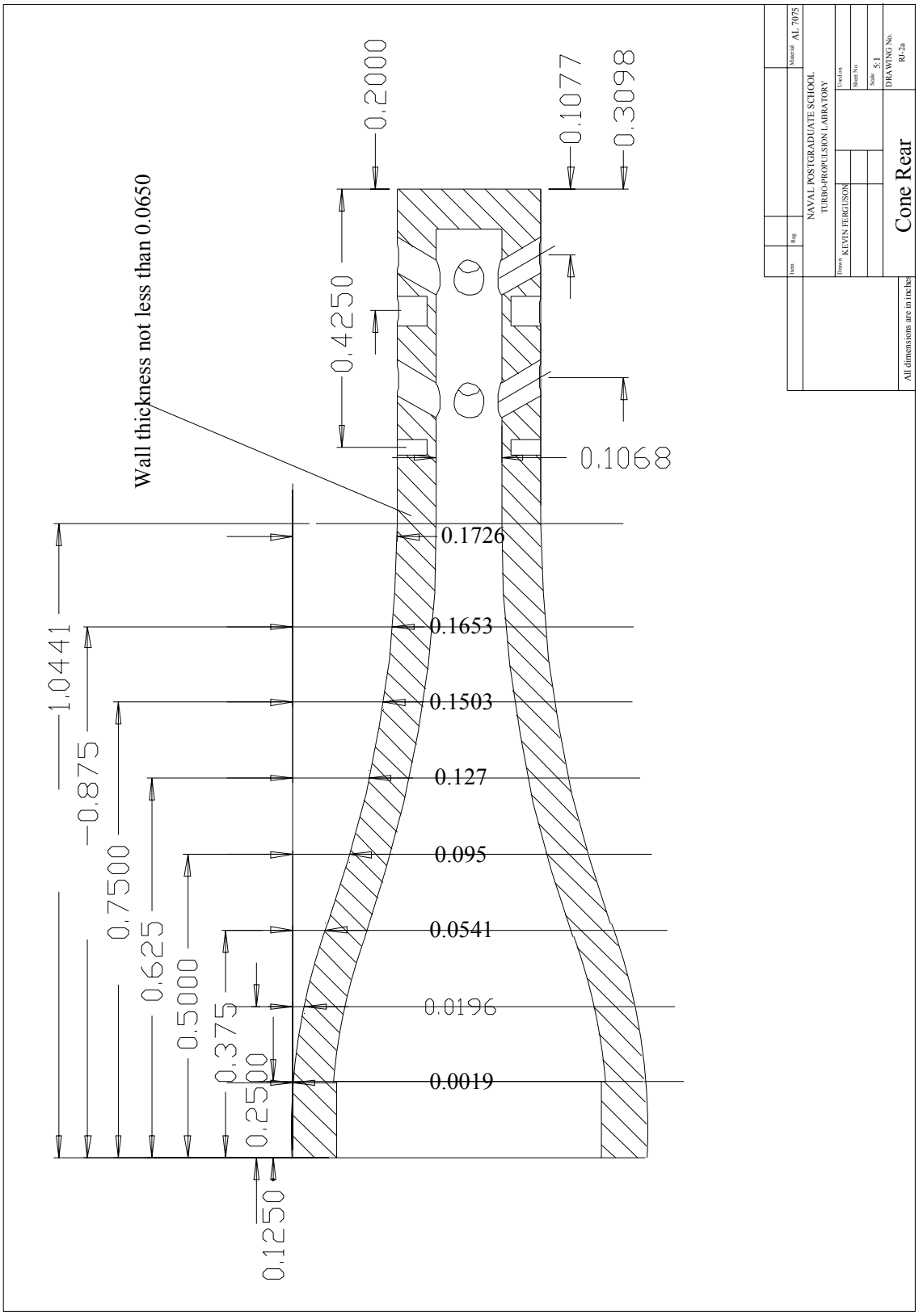

Figure 46. Part drawing: Contour of rear of inlet nose cone (RJ-2a)

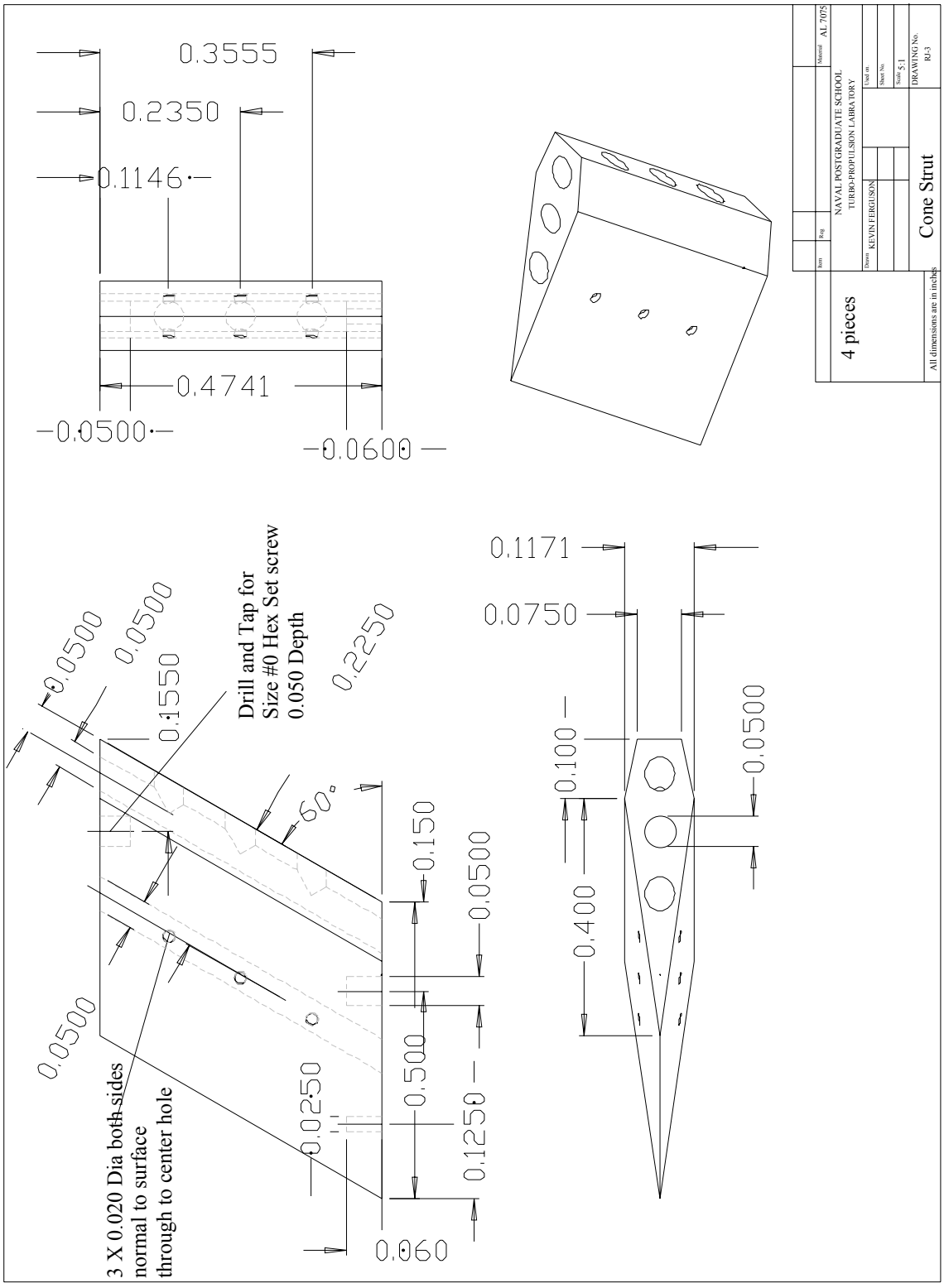

Figure 47. Part drawing: Ramjet fuel injecting strut (RJ-3)

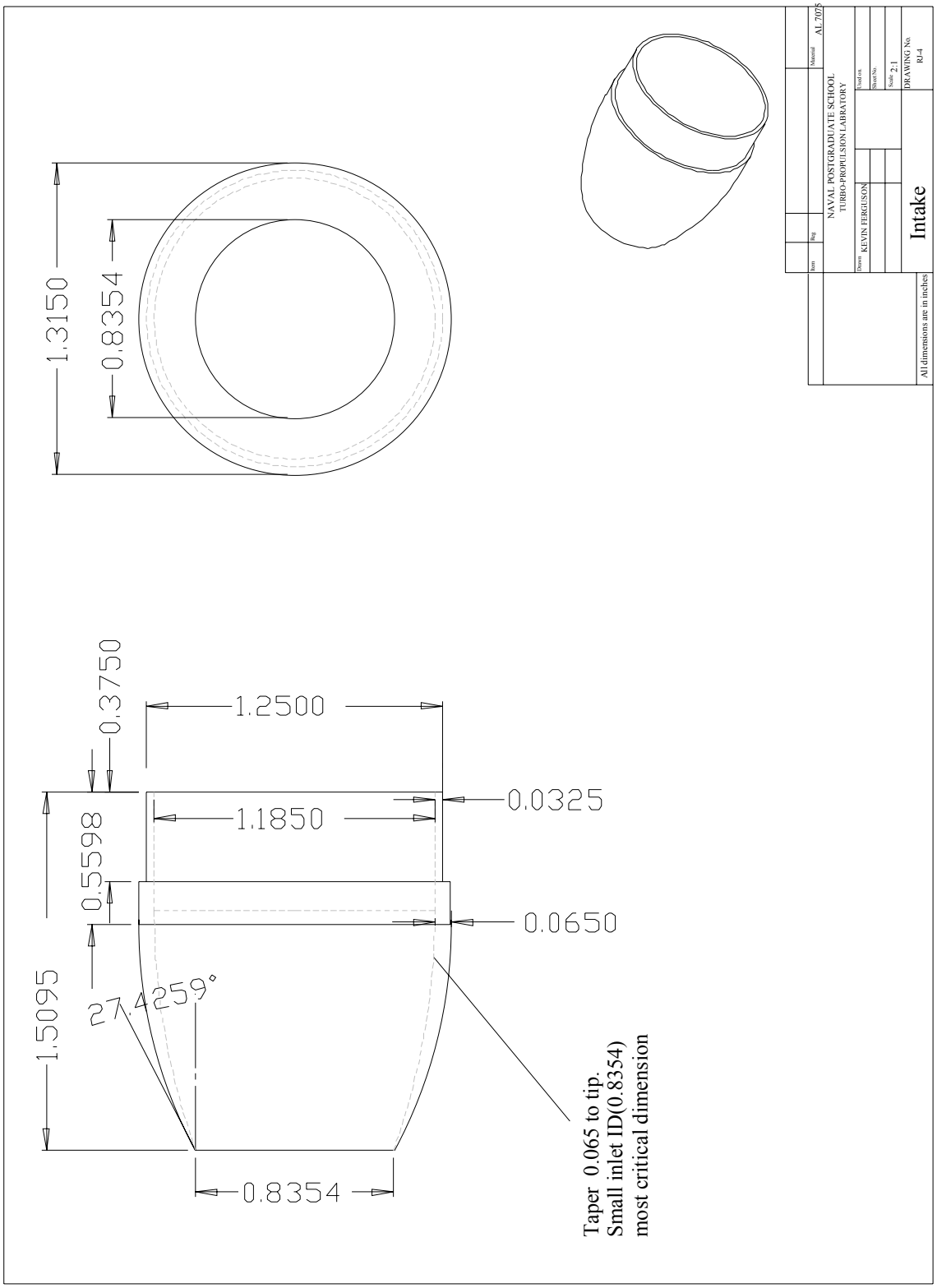

Figure 48. Part drawing: Ramjet intake (RJ-4)

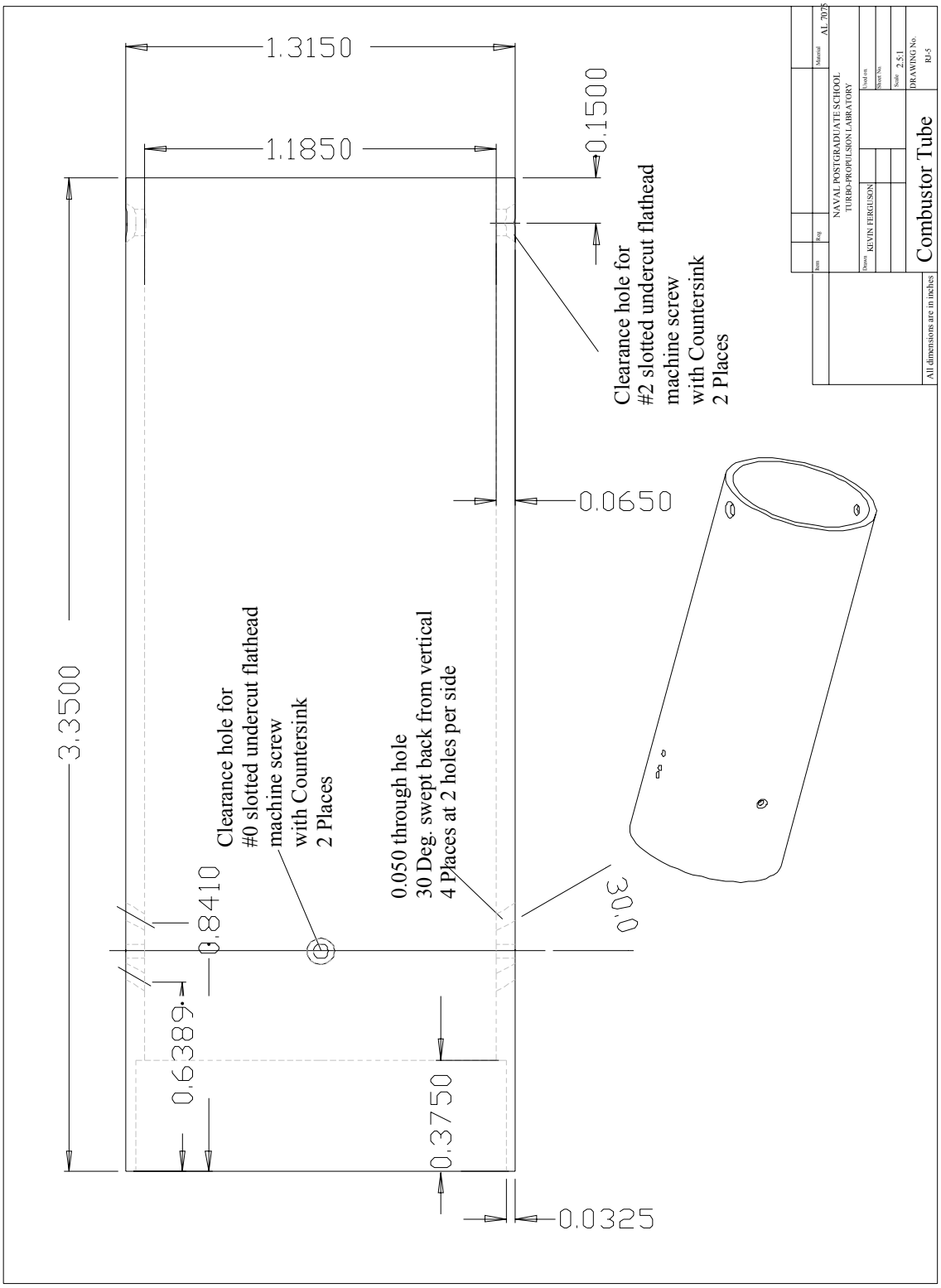

Figure 49. Part drawing: Ramjet combustion chamber (RJ-5)

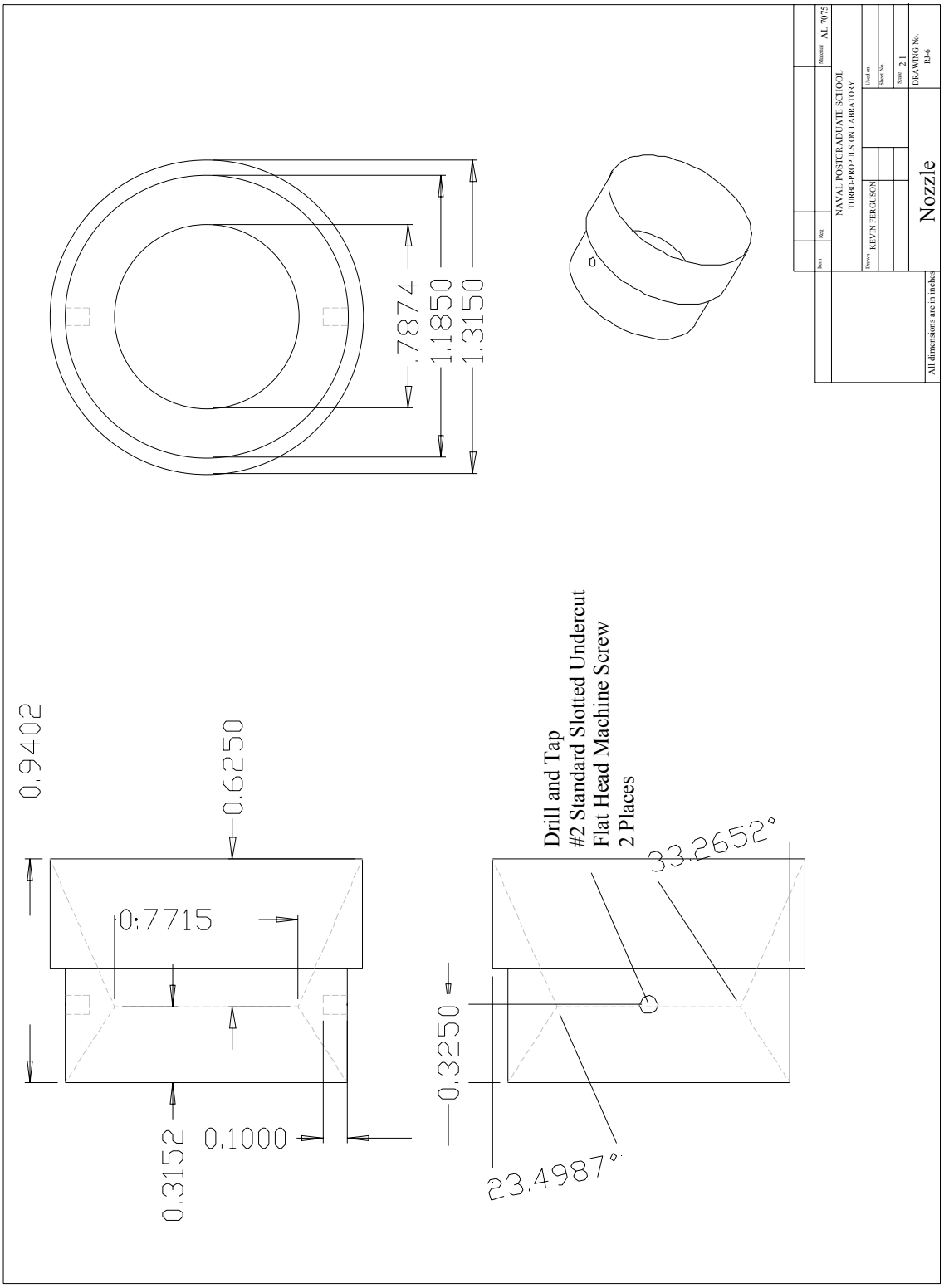

Figure 50. Part drawing: Ramjet nozzle (RJ-6)

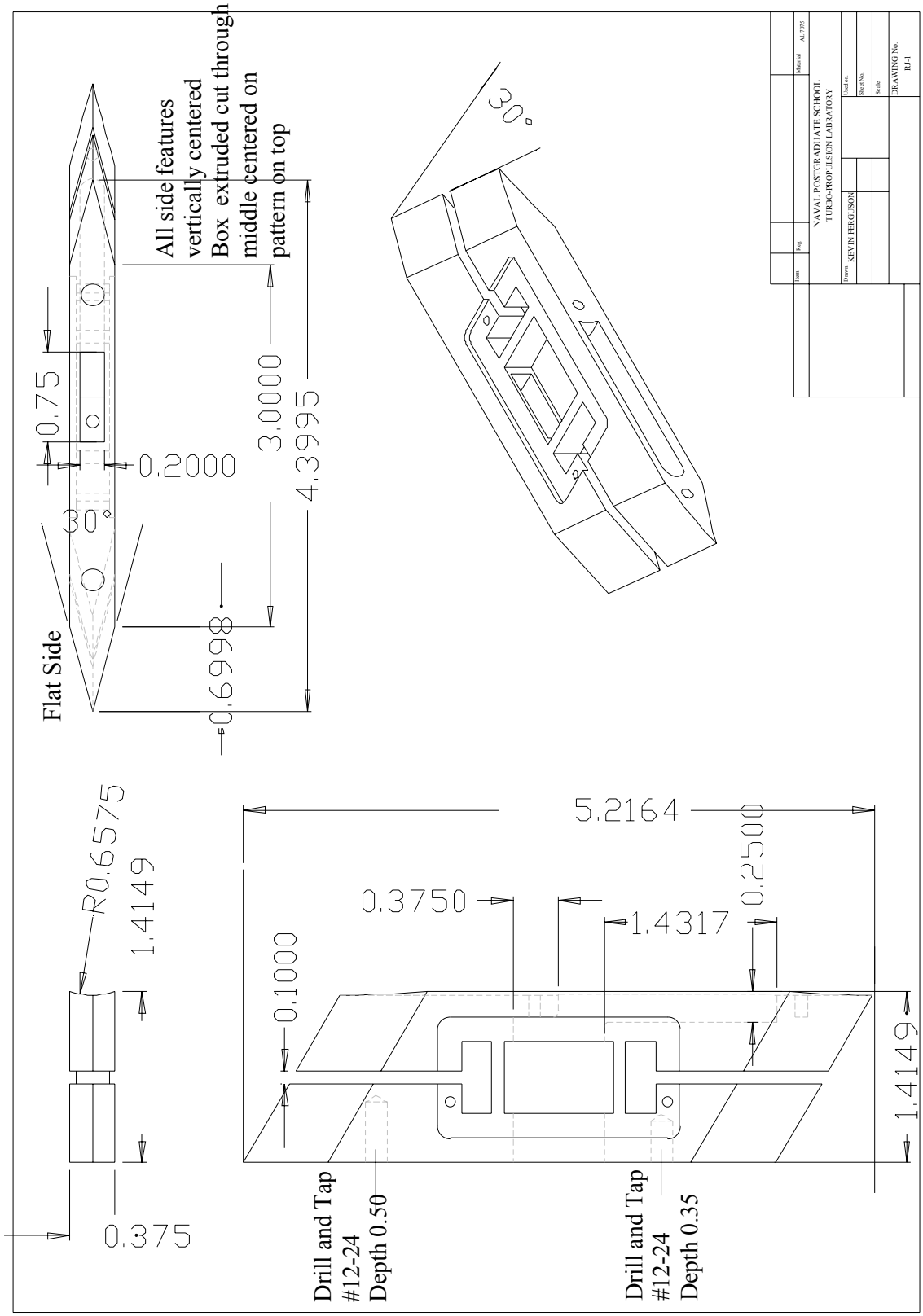

Figure 51. Part drawing: Ramjet wind tunnel strut (RJ-7)

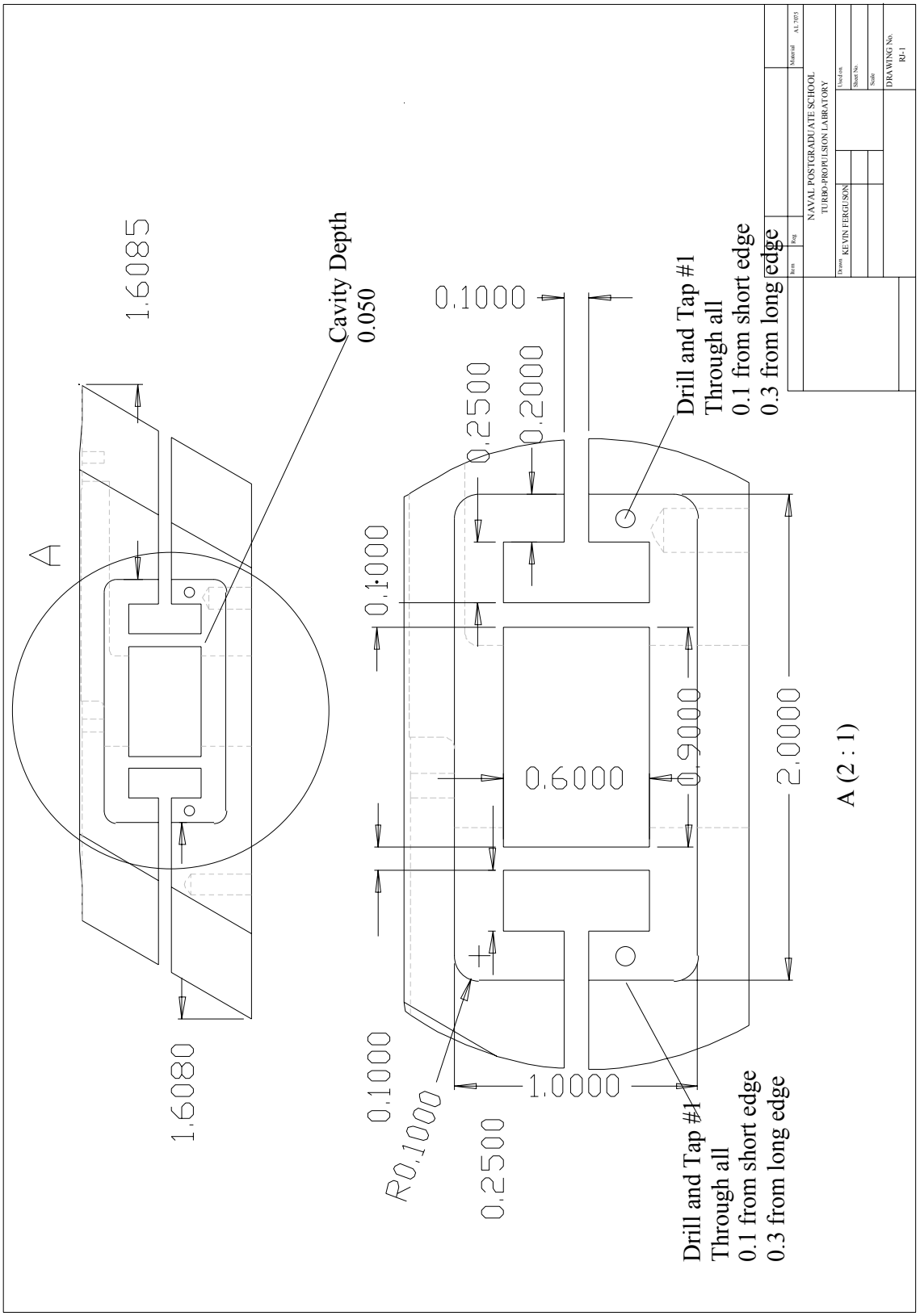

Figure 52. Part drawing: Ramjet wind tunnel strut (RJ-7a)

THIS PAGE INTENTIONALLY LEFT BLANK

APPENDIX F. LIST OF FASTENERS

Nozzle to Tube

(2) #2-56 Slotted Undercut Flat Head Machine Screw 0.160in total length

Strut to Tube

(2) #0-80 Set Screw 0.11in length (0.115 max) Stainless Steel

(2) #0-80 Slotted Undercut Flat Head Machine Screw 0.11 length (0.115 max)

(4) 0.025 Dia pins 0.0950 length (0.10 max) Stainless Steel

Strut to CB

(4) 0.025 Dia pins 0.0950 length (0.10 max) Stainless Steel

(4) 0.050 Dia pins 0.0950 length (0.10 max) Stainless Steel

Tube to Holder

(2) 0.050 Dia pins 0.30 length (.27min .315max)

(2) #3-48 Machine Screw 0.315 (.275min) thread length Rounded or Pan Head

Holder to Tunnel

(4) #12-24 Machine Screws 2 ½“ length

Loctite® E-120HP Hysol® Epoxy Adhesive

THIS PAGE INTENTIONALLY LEFT BLANK

APPENDIX G. GRIDED PROCEDURES

Enter input PLOT3D grid filename:
> *.grd

Enter itin and itout:
> 4 (3D formatted plane), 2 (3D formatted whole)

> 1 (Go to single grid menu)

> 2 (interchange J and K families)

> 1 (Yes, further operations)

> 8 (rotate about axis)

> 1 (positive x axis)

> 90 (degrees of rotation)

> 1 (Yes, further operations)

> 14 (Add extra planes to 2D grid to form 3D grid for '2D' or axisymmetric' option in OVERFLOW)

> 3 (generate 'axisymmetric grid' in J-K)

> 0 (No, further operations)

Enter output file
> grid.for

> 0 (single output format)

THIS PAGE INTENTIONALLY LEFT BLANK

APPENDIX H. OVERFLOW INPUT FILES

```
$GLOBAL
    CHIMRA= .F.,   NSTEPS=40000,   RESTRT= .F.,   NSAVE =1000,
    NQT   = 202,   NFOMO=1000,
    $END
$FLOINP
    ALPHA =0,  FSMACH= 4.00,  REY   = 2.3E6,  TINF  = 122.400,
    XKINF=.0001, RETINF=0.1, GAMINF=1.4,
    $END
$VARGAM
    IGAM=0,
    $END
$GRDNAM
    NAME = 'Axi-symmetric nozzle inlet',
$END
$NITERS
    $END
$METPRM
    $END
$TIMACU
    ITIME=1,
    DT=.5,
    CFLMIN=0,
    CFLMAX=1,
    $END
$SMOACU
    $END
$VISINP
    VISC =.T.,
    CFLT = 1,
    ITERT = 3,
    $END
$BCINP
    NBC   =  11,
    IBTYP =  5,  5,  5,  5,  5, 32, 32, 22, 16, 16, 61
    IBDIR = -1,  1, -2,  2,  2, -2, -1,  3,  1,  2,  1
    JBCS  =101,391,101,101,  1,  1, -1,  1,  1,261,102
    JBCE  =101,391,391,391,261, -1, -1, -1,  1, -1,390
    KBCS  = 61, 61, 61, 67,  1, -1,  1,  1,  1,  1, 62
    KBCE  = 67, 67, 61, 67,  1, -1, -1, -1, -1,  1, 66
    LBCS  =  1,  1,  1,  1,  1,  1,  1,  1,  1,  1,  1
    LBCE  = -1, -1, -1, -1, -1, -1, -1,  1, -1, -1, -1
$END
$SCEINP
$END
```

Figure 53. Representative OVERFLOW input file

THIS PAGE INTENTIONALLY LEFT BLANK

APPENDIX I. FAST IMAGES

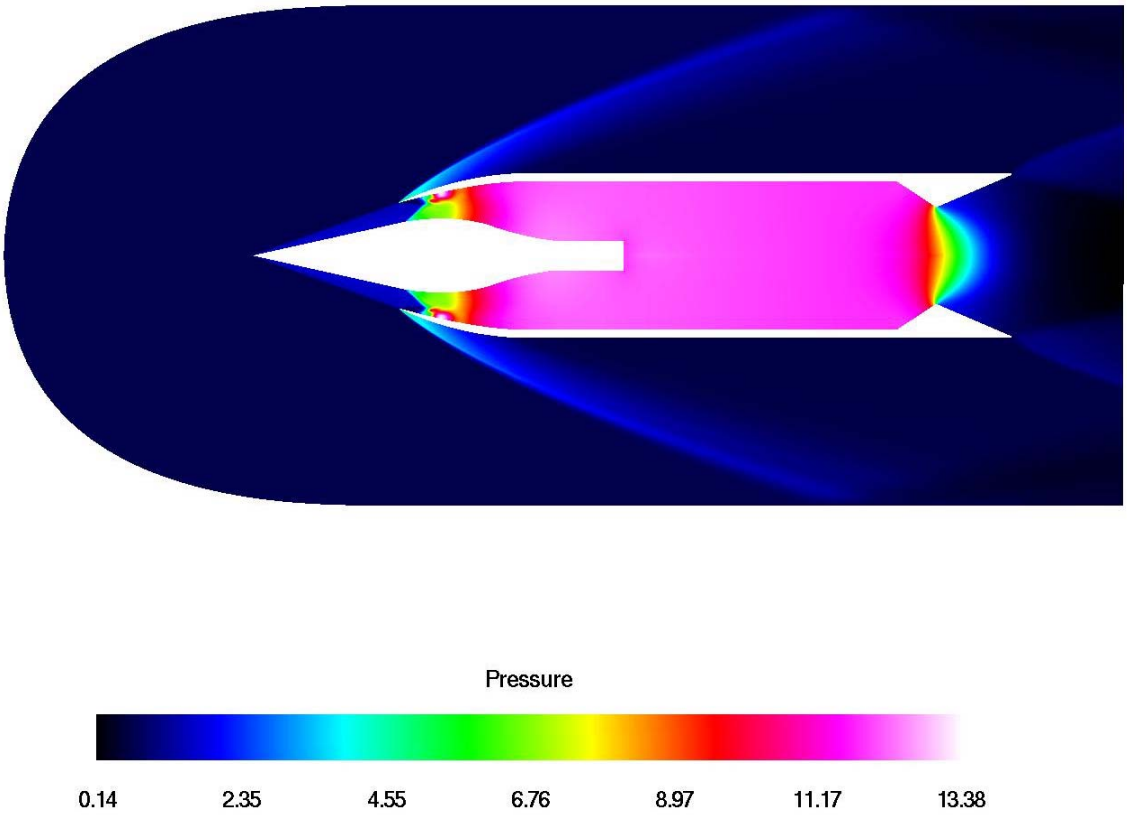

Figure 54. FAST image of pressure contours of viscous solution

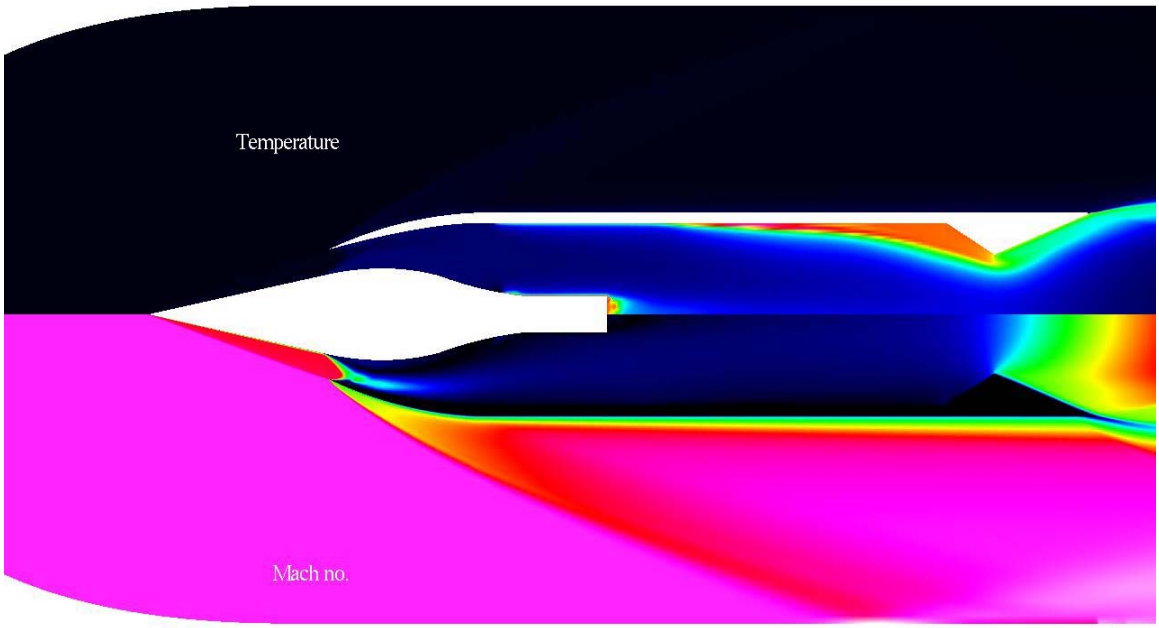

Figure 55. FAST image of Mach number (bottom) and temperature profile (top)

THIS PAGE INTENTIONALLY LEFT BLANK

LIST OF REFERENCES

1. Hackaday, G., *Thrust Augmentation for a Small Turbojet Engine*, Master's Thesis, Department of Aeronautics and Astronautics, U.S. Naval Postgraduate School, Monterey, CA, March 1999.

2. Piper, R.H., *Design and Testing of a Combustor for a Turbo-ramjet for UAV and Missile Applications*, Master's Thesis, Department of Aeronautics and Astronautics, U.S. Naval Postgraduate School, Monterey, CA, March 2003.

3. Kurzke, J., *GASTURB 9.0 for Windows: A Program to Calculate, Design and Off Design Performance of Gas Turbine Engines,* 2001.

4. Sims, J.L., *Tables for Supersonic Flow Around Right Circular Cones at Zero Angle of Attack,* National Aeronautics and Space Administration, Office of Scientific and Technical Information, 1964.

5. Zucker, R.D., *Fundamentals of Gas Dynamics,* pp. 380-401, Matrix Publishers, INC., 1997.

6. Buning, P. G., et. al., *OVERFLOW User's Manual*, NASA Ames Research Center, March 1998.

THIS PAGE INTENTIONALLY LEFT BLANK

INITIAL DISTRIBUTION LIST

1. Defense Technical Information Center
   Ft. Belvoir, Virginia

2. Dudley Knox Library
   Naval Postgraduate School
   Monterey, California

3. Prof Max Platzer
   Chairman, Department of Aeronautics
   Naval Postgraduate School
   Monterey, CA

4. Prof Garth V. Hobson
   Naval Postgraduate School
   Monterey, CA

5. Prof Raymond P. Shreeve
   Naval Postgraduate School
   Monterey, CA

6. Naval Air Warfare Center Aircraft Division
   Propulsion and Power Engineering
   Patuxent River, MD
   ATTN: C. Georgia, Code 4.4

7. Naval Air Warfare Center Weapons Division
   China Lake, CA
   ATTN: J. Moore, Code 477400D

8. Kevin M. Ferguson
   ENS, USNR
   Langhorne, PA